NEUTRON SPECTRAL EFFECT ON MICROELECTRONIC PERFORMANCE RESPONSE

THESIS

Wade Kloppenburg

AFIT-ENG-MS-20-90210

DEPARTMENT OF THE AIR FORCE
AIR UNIVERSITY

AIR FORCE INSTITUTE OF TECHNOLOGY

Wright-Patterson Air Force Base, Ohio

AFIT-ENG-MS-20-90210

NEUTRON SPECTRAL EFFECT ON MICROELECTRONIC PERFORMANCE RESPONSE

THESIS

Presented to the Faculty

Department of Nuclear Engineering

Graduate School of Engineering and Management

Air Force Institute of Technology

Air University

Air Education and Training Command

in Partial Fulfillment of the Requirements for the

Degree of Master of Science in Nuclear Engineering

Wade Kloppenburg, B.S.

March 26, 2022

AFIT-ENG-MS-20-90210

NEUTRON SPECTRAL EFFECT ON MICROELECTRONIC PERFORMANCE RESPONSE

THESIS

Wade Kloppenburg, B.S.

Committee Membership:

James Petrosky, Ph.D
Chair

George Peterson, Ph.D
Member

Maj. James Bevins, Ph.D
Member

AFIT-ENG-MS-20-90210

Abstract

It is well known that neutron radiation has an effect on bipolar junction transistor performance. Less is known, however, of a difference in response if the spectrum of neutrons is from a pulsed thermonuclear or pulsed fission source, where the neutron spectrum is substantially different. This research strives to characterize performance changes due to relevant fluxes of pulsed neutrons with thermonuclear or pulsed fission spectra. This research utilized three neutron environments for analysis; a steady-state thermalized fission source at the Ohio State University Research Reactor, a pulsed deuterium tritium fusion source at the National Ignition Facility, and a pulsed thermonuclear plus prompt fission spectrum developed using an energy tuning assembly on the ATHENA apparatus at the National Ignition Facility. 2N2222 npn bipolar junction transistors were irradiated in each environment. Each environment possessed markedly different total fluence, neutron spectra, and temporal profiles. Measuring differences in transistor performance can establish potential differences due to the relevant source parameters. Measurements used for comparing performance included the base-collector junction current-voltage, based-collector capacitance-voltage characteristics, and device gain degradation. Dynamic base-collector current was collected at the National Ignition Facility to observe the effects of the prompt irradiation and subsequent dynamic annealing during and immediately after irradiation. Post-irradiation characterization measurements were obtained for each irradiated transistor and statistically analyzed to determine changes in operation. Little change was detected in steady-state operation of the base-collector junction after the devices were de-soldered from the circuit, but evidence in the dynamic data and capacitance measurements establish differences affected by the radiation environment.

Table of Contents

Page

List of Figures

List of Tables

NEUTRON SPECTRAL EFFECT ON MICROELECTRONIC PERFORMANCE RESPONSE

I. Introduction

1.1 Research Objectives

This research is focused on the study of radiation effects on microelectronic devices in pulsed neutron environments. The experiment involved exposing Motorola 2N2222 bipolar junction transistors (BJTs) to fluences of greater than 10^{12} n/cm^2 1 MeV(Si) in three environments, with vastly different spectra and temporal profiles. The neutron environments used for comparison were the central cavity of the Ohio State University Research Reactor (OSURR), which provides a steady-state thermalized fission spectrum and two locations on the ATHENA platform at the National Ignition Facility (NIF). Irradiation exposures on the ATHENA platform were performed at an external arm of the ATHENA apparatus, hereafter referred to as "external", or internal to an energy tuning assembly (ETA), hereafter referred to as "internal". External exposures provide a pulsed characteristic DT fusion energy spectrum as provided by the NIF deuterium-tritium (DT) source. Internal exposures provide a pulsed moderated spectrum using an ETA designed to match a spectrum; in this case a thermonuclear plus prompt fission spectrum (TN+PFS) [1, 5]. This work involved statistically analyzing the current and capacitance measurements on 2N2222 transistors before and after irradiation, and comparing the differences in performance to transistors irradiated to the same approximate fluence at the OSURR.

1.2 Problem Statement

It is well known that neutron radiation has an effect on BJT operation [6, 7, 8, 9, 10, 11]. Less is known, however, of the difference between a reactor environment and a combined TN+PFS environment. This experiment strives to characterize that difference and analyze the influence of a TN+PFS environment on transistor performance.

The damaging effects of high energy neutrons in microelectronics is based upon non-ionizing energy loss (NIEL) caused by classical collisions between the neutrons and atoms in the electronic medium. Although one can adjust the predicted damage from different neutron energies by accounting for the NIEL damage throughout the kinetic energy released per unit mass (KERMA), in a high flux neutron irradiation environment the damage may be affected by the local environment during the evolution of the damaged species [12]. Evaluating this is difficult due to the limited way in which to produce a high flux of neutrons with differing spectra and inability to make measurements (especially those based upon spectroscopy) during or immediately after irradiation.

This research uses three environments to measure the short and long term performance changes due to neutrons of different spectra and flux, and uses these measurements to analyze the effects of the spectrum on the overall parameters affecting performance.

1.2.1 Research Questions

This research serves to answer the following questions:

1. Do silicon BJTs irradiated with the same 1MeV(Si) equivalent neutron fluence but with a different energy spectrum respond differently?

2. Can species evolution be observed in dynamic data extracted from devices irradiated in a short neutron pulse experiment on the ATHENA platform?

1.2.2 Hypotheses

- Si BJTs irradiated with a high flux of neutrons will have the same post-irradiation damage characteristics, but the dynamic data will be different due to a different environment during the damage evolution.
- The ATHENA platform, used with a pulsed fusion source at the NIF, will provide sufficient evidence to indicate differences in the TN spectrum, the TN+PFS, and the steady state thermal spectra.

II. Background and Literature Review

The ATHENA II experiment was designed to demonstrate a platform for the evaluation of microelectronic devices exposed to relevant neutron spectra. The ATHENA apparatus allows for exposures to a pulsed TN neutron spectrum from a compressed DT source, and a spectrally modified relevant pulsed TN+PFS neutron spectrum [5]. This platform has been engineered via successive development through transport modeling and testing for 2+ years.

There has been much research to assess radiation effects on electronics because of their ubiquitous use. As early as the 1950's, George Messenger performed experiments assessing the effects of neutron irradiation on semiconductors [13]. Many publications have been published correlating neutron effects on microelectronic performance in various relevant technologies and environments [8, 11]. Applications of the methods developed in the past have been applied to experiments more recently with heavy ions [6] and to develop comparative metrics between experimental conditions and relevant environments [7]. All of this work is important to the radiation effects community for this and future research.

With a ban on nuclear weapon testing and the closing of the Sandia Pulsed Reactor, a gap exists in capability to create pulsed neutron radiation for evaluation of new materials and electronics in relevant environments. Using the NIF and an ETA, a pulsed neutron environment can be created and moderated to a desired spectrum. For this research, the ATHENA II platform is used to expose electronics to a TN and TN+PFS relevant to national security needs [5].

2.1 Neutron Environments Used in the Present Research

This research focuses on two experiments that explore three separate environments in the course of this experiment: a steady-state thermalized fission spectrum, a pulsed, near-monoenergetic TN spectrum, and a pulsed TN+PFS.

2.1.1 OSURR Steady-State Thermalized Neutron Fission Spectrum

The OSURR is a pool-type reactor with beam ports and dry tubes for irradiation facilities [14]. It operates on 19% enriched U_3Si_2 for fuel with light water as its moderator and primary coolant. The OSURR is primarily an academic facility, commonly used for nuclear engineering research and education [14, 15, 16, 17]. It operates at thermal powers up to 500 kilowatts with maximum neutron flux in the central facility at approximately 1.7×10^{13} n/cm^2/s.

The OSURR pneumatic transport "rabbit" facility was used to deliver the transistors to the reactor's central cavity for irradiation in a fission neutron spectrum. The rabbit tube uses a vacuum system, bringing a sample bottle into the reactor and extracting it, allowing for sample irradiation without interrupting normal reactor operations [17, 18]. Figure 1 shows the spectrum provided by the OSURR at 7 kW power.

2.1.2 NIF Monoenergetic Pulsed Neutron Fusion Spectrum

The NIF generates a pulsed fusion neutron source using high powered lasers targeting a small deuterium-tritium (DT) pellet. Using the lasers to energize the DT pellet, fusion is initiated creating the reaction:

$$ {}^{2}_{1}D + {}^{3}_{1}T \rightarrow {}^{4}_{2}\alpha + {}^{1}_{0}n + 14.1MeV. \tag{1} $$

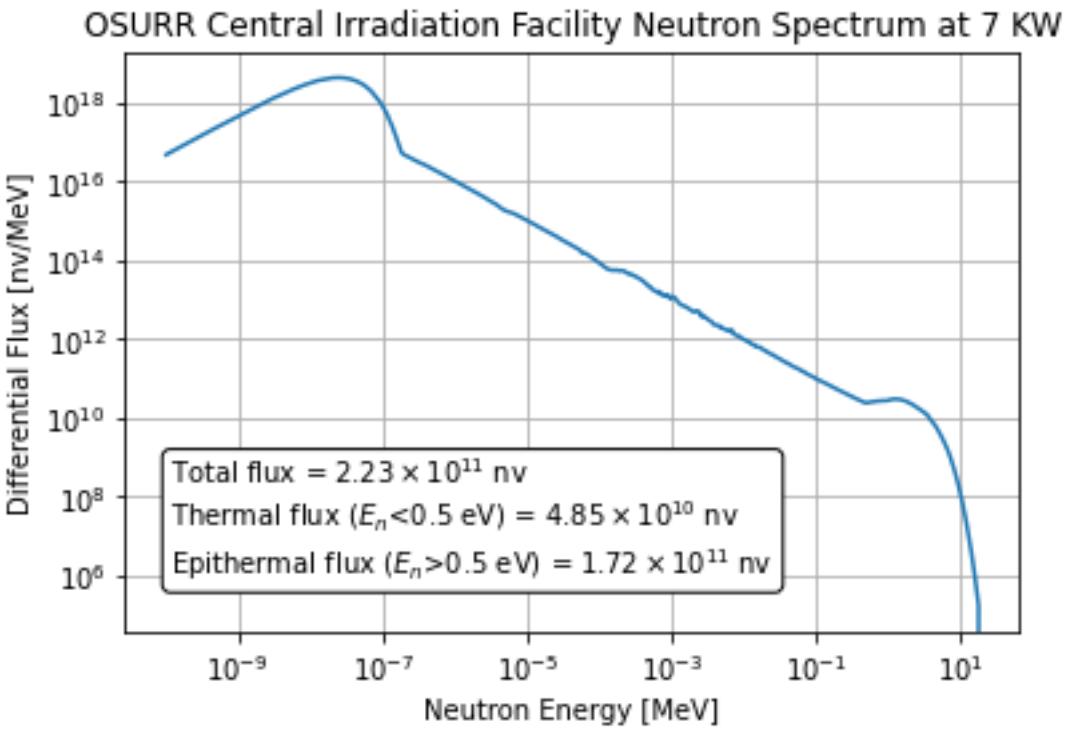

Figure 1: Differential flux measured at the OSURR Central Irradiation Facility.

This reaction provides a source of neutrons at approximately 14.1 MeV. Figure 2 presents the NIF's neutron spectrum as measured using the neutron time-of-flight data against the theoretical spectrum based on an 8.8 keV ion temperature plasma [1]. DT fusion produces gammas with a branching ratio of $4.2 \pm 2.0 \times 10^{-5}$, a limited contribution to radiation dose, making it an ideal source for measuring the effects of neutron irradiation on a microelectronic device without the impact of gamma radiation on the device [1].

2.1.3 NIF Plus ETA Pulsed Neutron Thermonuclear+Prompt Fission Neutron Spectrum

A TN+PFS is the superposition of a DT fusion spectrum with a fission spectrum released in a very short, sub-microsecond, timeframe. Figure 3 shows the neutron spectrum released from a thermonuclear weapon detonation [2]. The DT fusion re-

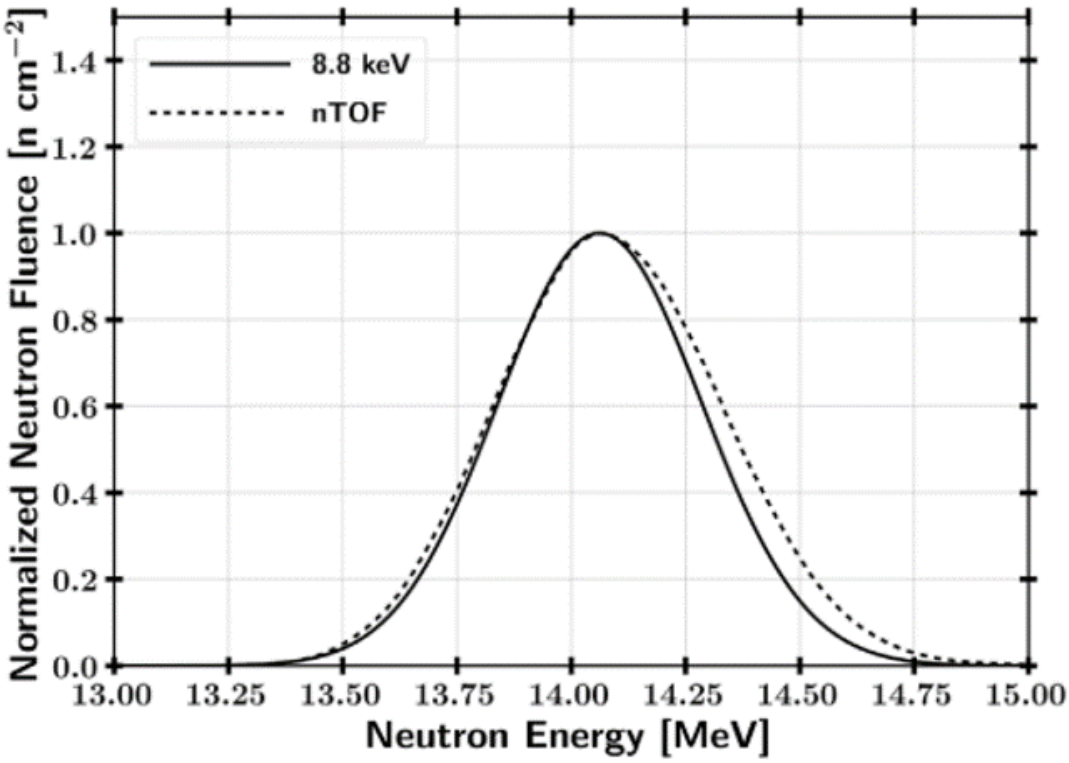

Figure 2: Neutron spectrum from NIF measured using neutron time of flight as compared to a theoretical spectrum of 8.8 keV ion temperature plasma [1].

action 14 MeV neutrons are evident, with a significant portion of a fission spectrum clearly superimposed in the thermal region.

To provide a TN+PFS, ATHENA II uses an ETA, Figure 4, in order to moderate the incoming neutrons to achieve the desired spectrum. The ETA is conical to best fit to the spherical divergence of neutrons from the NIF DT source. It consists of layers of zirconium, tungsten, graphite, and Delrin to moderate the DT neutrons to match a desired spectrum [1]. A cylindrical cavity provides a test space interior to the ETA, with a drawer built into the side for access to the environment inside and placement of activation foils for measuring the neutron spectrum. A shelf is also built on the exterior of ATHENA to mount samples for access to the unmoderated TN NIF spectrum. Neutron activation foils were used during the experiment to determine the

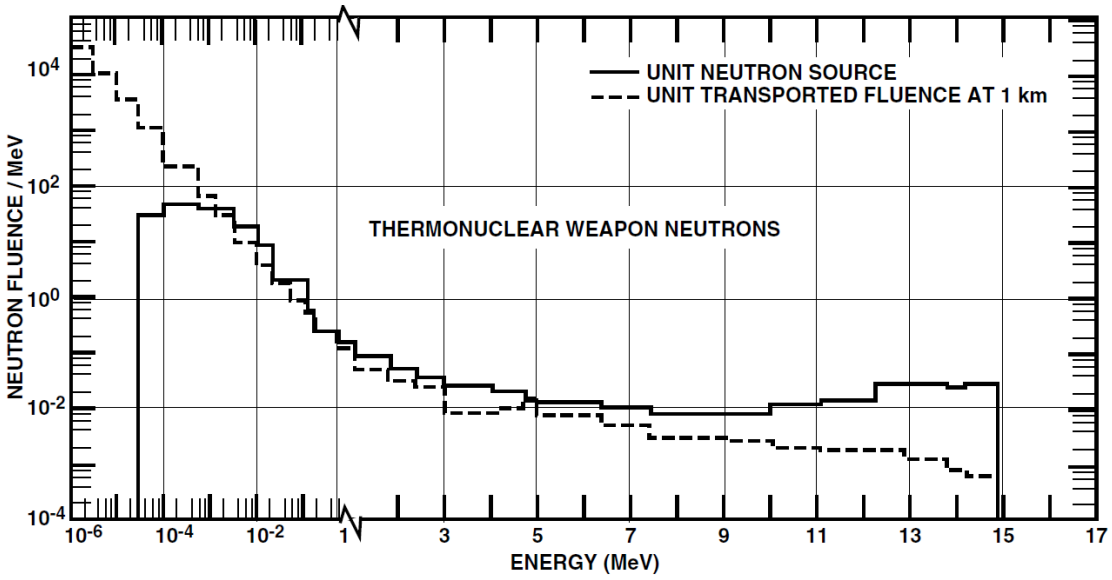

Figure 3: Neutron spectrum from a thermonuclear weapon detonation [2].

spectrum in each region. Figure 5 is a normalized spectrum of both interior and exterior locations of ATHENA. On the exterior of ATHENA the "fission" portion, $E \leq 12MeV$, is very low in comparison to that of the drawer and inner cavity of ATHENA [1]. This indicates the success in ATHENA to tune the neutron spectrum near a TN+PFS. Furthermore, the back of the ETA provides access for cabling so that microelectronic devices on the ATHENA platform can be actively monitored during the pulse.

2.1.4 1 MeV Si Neutron Equivalence Methodology

Neutron interactions with matter vary with spectra [10]. Multiple environments are used in this research to explore the effects of this, but a metric is needed to compare neutron damage between spectra and platforms. The 1 MeV(Si) $\frac{n}{cm^2}$ fluence equivalence is often used to meet this need [3, 19, 20, 21]. This is calculated by equation 2 [3].

$$\Psi_{eq.Eref.mat} = \frac{\int_0^\infty \Psi(E) F_{D.mat}(E) dE}{F_{D.Eref.mat}} \tag{2}$$

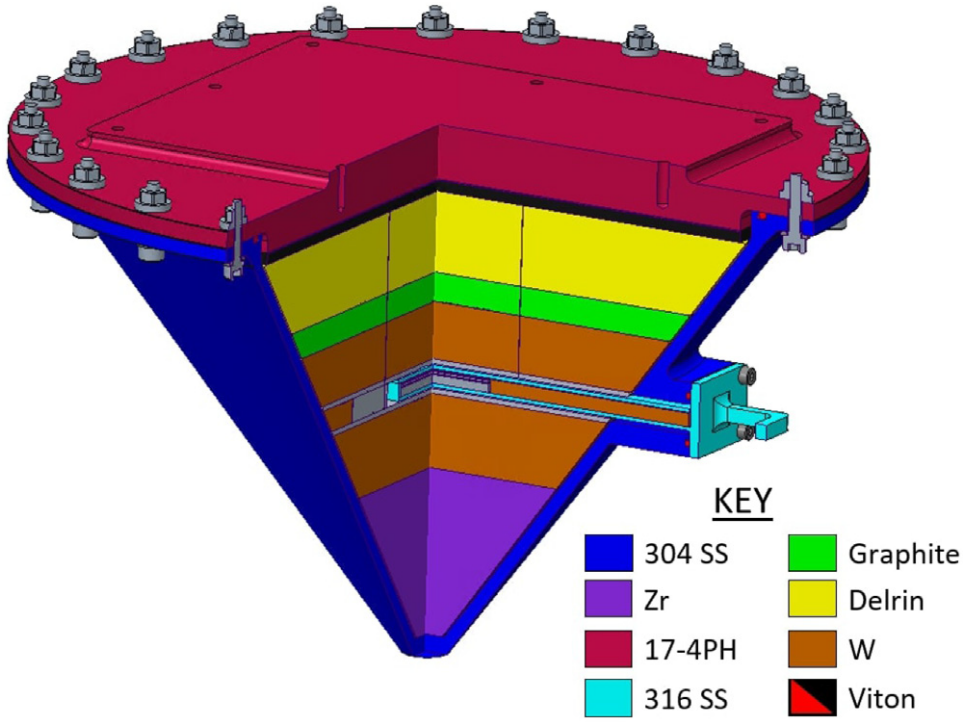

Figure 4: The ATHENA energy tuning assembly. Layers of material moderate neutrons to a TN+PFS in the interior cavity.

In Equation 2, $\Psi(E)$ represents the incident neutron fluence as a function of energy, $F_{D.mat}$ is the neutron displacement damage function, and $F_{D.Eref.mat}$ is the displacement damage reference value for the designated material. Figure 6 shows the neutron displacement damage function for silicon, based on the 1 MeV(Si) fluence.

The 1 MeV equivalence accounts for the spectrum in which a target is irradiated, but some challenges are presented. The damage KERMA used to evaluate 1 MeV equivalence is based on a thermal neutron spectrum and the temporal profile over which the irradiation is received. Over long irradiation periods (e.g. low flux), defects have time to anneal, removing them from the environment before a subsequent point defect is formed. In a shorter temporal span between interactions (e.g. high flux), interactions may occur before any thermal annealing is complete, changing the environment in which annealing occurs. In the present research, it is

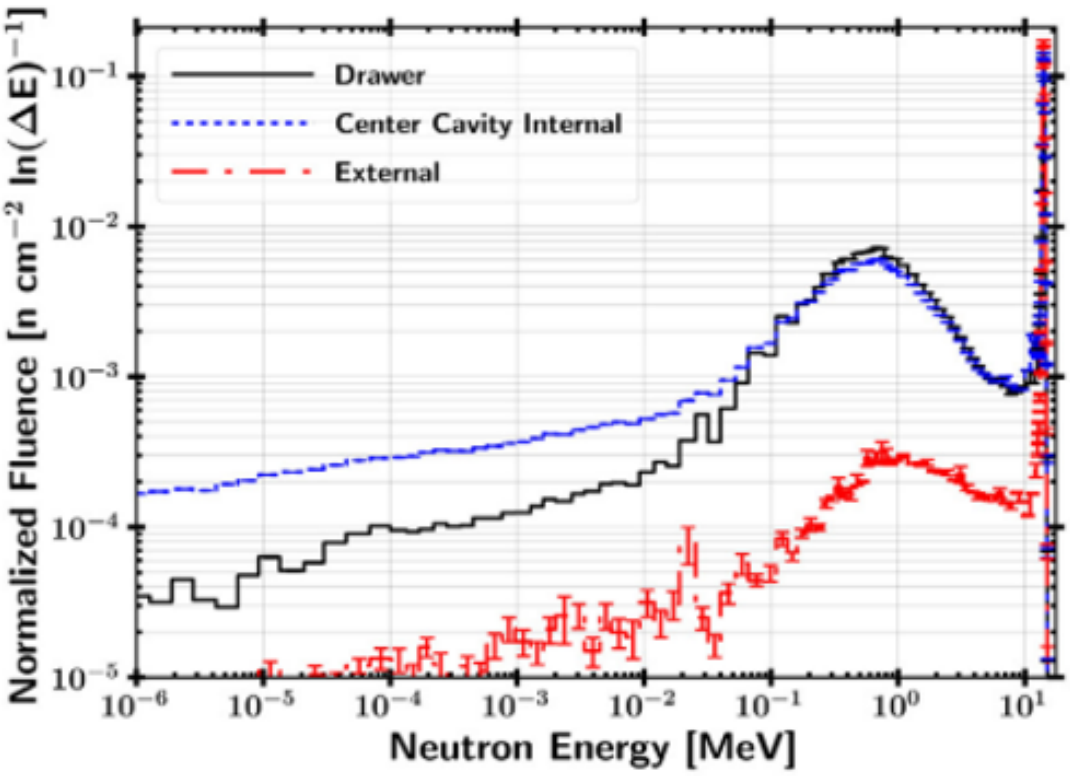

Figure 5: Normalized neutron spectrum from ATHENA ETA [1].

this concept related to 1 MeV equivalence which can be practically evaluated. By comparing transistor performance, irradiated in different environments, at the same 1 MeV equivalent fluence, the usefulness of the parameter itself is evaluated.

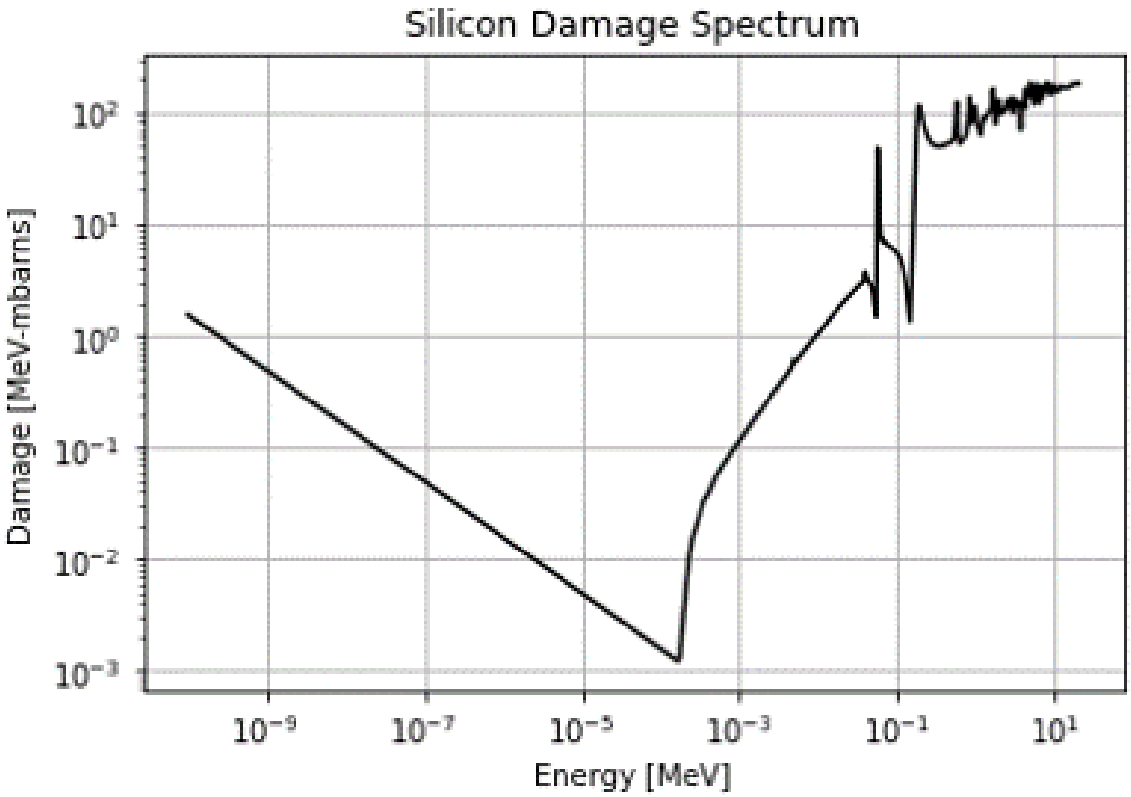

Figure 6: Kinetic energy released per unit mass for silicon [3].

2.2 Fundamental Operation of the Bipolar Junction Transistor

To evaluate the effects of neutron exposure on a microelectronic device, 2N2222 bipolar junction transistors (BJT) were chosen, as they are well characterized in past neutron irradiation experiments and are susceptible to neutron damage [7, 8, 9]. BJTs are solid state, microelectronic devices that consist of three regions doped to provide either excess electron (n-type) or hole (p-type) conductivity. BJTs come in two varieties, npn or pnp. The pn junctions between regions initially allow for high resistance to current from the collector to emitter of the BJT. By introducing current to the base of the BJT, it increases the conductivity of the region, allowing the passage of current from the collector to the emitter like an electronic gain switch. Operation of a BJT in forward active, common emitter configuration (the most commonly used

configuration and most affected by neutron damage) is shown in Figure 7. 2N2222 BJTs are npn doped transistors, where the emitter is highly n doped, the base is p doped, and the collector is lightly n doped. The currents at the contacts of the transistor are related via the equation 3 [22].

$$I_e = I_b + I_c \tag{3}$$

In Equation 3, I_e is the emitter current, I_b is the base current, and I_c is the collector current.

For a BJT to operate in forward active mode, the junction between the base and collector (B-C) must be reverse biased, and the junction between base and emitter (B-E) must be forward biased [4][22]. When biased in this way, such that $V_c > V_b > V_e$, the transistor will appear to have a current gain at the emitter. Current gain (β) is defined by the ratio of current at the collector to current at the base, as in Equation 4 [22].

$$\beta = \frac{I_c}{I_b} \tag{4}$$

A BJT can operate in reverse, or inverted mode, with current entering the transistor through the base and emitter and exiting through the collector. To do this, B-C must be forward biased and B-E must be reverse biased [23]. Current will flow through the BJT, but not as efficiently as in forward active mode. The common emitter current gain will be far less than in forward active mode [4].

Neutrons damage the silicon electronic structure, primarily through elastic collisions that result in dislocations in the silicon lattice. This damage causes a reduction in mobility of charge carriers in the transistor and creates traps within the lattice, reducing lifetime [13]. To compare changes in gain between environments, Bielejec

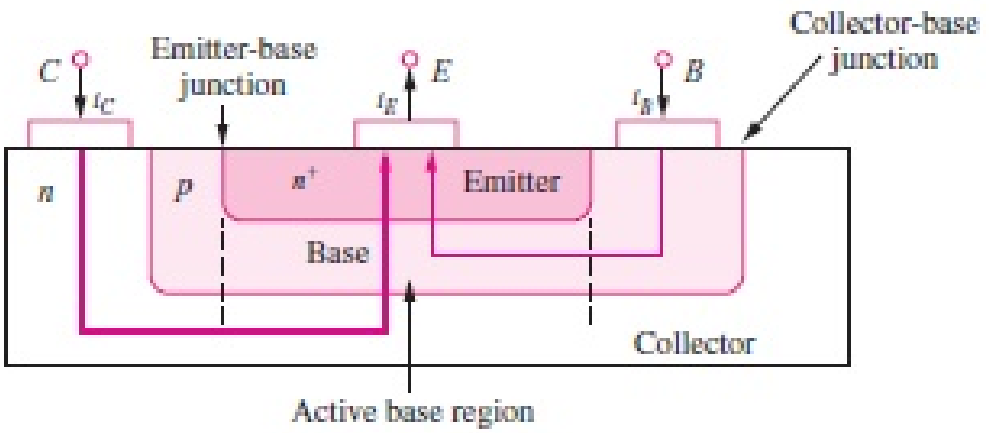

Figure 7: Simplified view of a BJT in forward active, common emitter configuration [4]

uses the metric "inverse gain degradation", defined in equation 5 [6]. Inverse gain degradation scales linearly with incoming radiation fluence [6, 7, 11, 13]. It provides a measure of the non-ionizing energy loss (NIEL) within the device because it is an indirect measure of the long-term, unannealed defects.

$$\Delta\left(\frac{1}{\beta}\right) = \frac{1}{\beta_\infty} - \frac{1}{\beta_0} \tag{5}$$

2.3 Statistical Methods Used for Analysis

To quantify performance changes due to neutron exposure, a statistical test was applied to the measured quantities. Only two devices were irradiated at each location in ATHENA and the measurements being performed do not ideally produce normal distributions of data. Therefore, non-parametric statistics are an appropriate analysis tool [24]. The Kruskal-Wallis test allows for testing two or more distributions simultaneously without an assumed data distribution. Its null hypothesis is that the data being compared are from the same distribution.

Much like a parametric analysis of variance method, the Kruskal-Wallis test detects differences between populations [24]. It accomplishes this by ranking data points as though all contributions originate from the same population. Probability is established and expressed by an H-statistic and a p-value that can be compared to the model's error [25]. It is common practice in statistics to assume an α value of 0.05 and a p-value less than α indicates a deviation between two or more distributions being tested [24].

Transistor measurements for current-voltage (IV) characteristics are not normally distributed, so in order to compare these, this research applied the Kruskal-Wallis statistics for comparisons. This research analyzes IV characteristics in three groups; a baseline of 16 unirradiated transistors, three OSURR irradiated transistors, and transistors from OSURR, NIF, TN+PFS irradiated at similar total fluence. Each group contains an unirradiated control, such that a deviation from the unirradiated operating state can be observed in the statistics.

III. Methodology

This section covers the experimental methodology used to characterize, irradiate, and assess the microelectronics used in the present research. The experiment itself focuses on shot N210526-001 at the NIF. Key requirements for the experiment were:

- a minimum output of 10^{16} neutrons in 4π from the target,
- use of the ATHENA energy tuning assembly,
- diagnostic circuitry including use of oscilloscopes for monitoring device dynamic performance,
- radiation diagnostics including: neutron time of flight (nTOF), nuclear activation diagnostics (NAD), gamma reaction history (GRH), and a neutron imager system (NIS), and
- timely removal of transistors and foil pack from ATHENA [5].

To reach these requirements, the NIF used 192 beams totaling 1.2 MJ energy targeting NIF's polar drive exploding pusher (PDXP) target. The PDXP target is a 4.0 mm diameter glow discharge plasma hydrocarbon plastic capsule with a wall thickness of 22 microns. The gas fill for the target was 65:35 DT at 8 atm pressure. This setup ideally provides the estimated 10^{16} fusion neutrons from the DT fusion reaction and 10^{12} 1 MeV(Si) incident on the transistors [26].

The ETA was fielded such that the narrow tip of the cone was at 60 mm from the PDXP target in order to maximize the neutrons flux to the transistors. Two transistors were mounted in the internal ETA position and two were mounted at the external ETA position to provide transistors with exposure to either the TN+PFS or

TN spectrum, respectively. The devices were powered such that they would remain in the forward active region during throughout the experiment.

Prior to shot N210526-001, a set of transistors were irradiated in the OSURR central cavity using the rabbit transfer system. These irradiations were used to set the baseline for performance changes expected in NIF shot N210526-001. They also provided baseline changes used to set circuit power and resistor values. Based upon transport models and NIF facility experience, shot N210526-001 was expected to deliver $> 10^{12}$ n/cm^2 1 MeV(Si) to the test devices [1]. To provide a baseline, the 2N2222 transistors were exposed to 10^{12}, 10^{13}, and 10^{14} n/cm^2 1 MeV(Si).

3.1 Precharacterization of 2N2222 devices

Prior to all irradiations, unirradiated transistors were measured to ensure any outliers in performance were removed from the test set. Current-voltage ($I_{BC}(V)$) and capacitance-voltage ($C_{BC}(V)$) were measured for the base-collector junction, and current and voltage measurements obtained such that a complete Gummel plot can be created and common emitter current gain could be determined. Capacitance measurements were obtained to derive the lifetime of carriers within the transistors.

IV measurements were made using a Keithley 237 Source Measurement Unit. Figure 8 is a diagram for the circuit used for these measurements. Cables were connected such that the high force was applied to the base of the transistor being measured, and low force was applied to the collector and connected to ground. The emitter was connected to ground. A Python program, in Appendix B, was used to communicate with the instrument through a GPIB bus to sweep voltage across the base and measures I_{BC}. The measurement was performed from -8 to 1 V, so that a full range of operating modes could be assessed, from breakdown through saturation. Resulting figures and analyses are in Chapter IV.

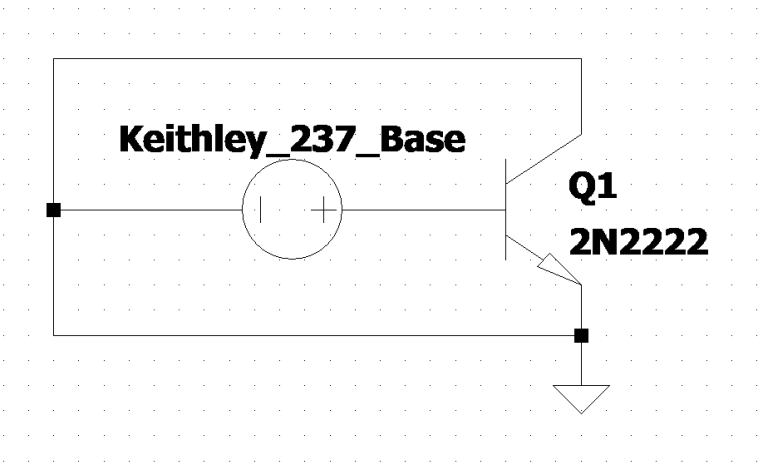

Figure 8: Circuit model for the current-voltage measurements. The Keithley 237 swept the base from -8 to 1 V, measuring current across the BC junction of the 2N2222 transistor.

Gain measurements were obtained in a similar fashion. The circuit diagram for gain measurements is shown in Figure 9. Using two Keithley 237 SMUs, a potential of 3.4 V was applied to the collector of the transistor, the base voltage was swept from 0 to 1 V in 5 mV increments, and the emitter was connected to a physical ground. These voltages ensure that the transistor is reverse biased at the BC junction and forward biased at the BE junction, putting the transistor into "forward active" mode [22].

The $C_{BC}(V)$ was measured using a Keithley 590 CV Analyzer. The base and collector were connected to the analyzer and the emitter was connected to ground. By measuring capacitance over a pn junction, one can calculate the lifetime of charge carriers within a device. Within a pn junction, two types of capacitance exist: diffusion capacitance (C_D) and junction capacitance (C_J), as defined in Equation 6 and 7, respectively [23].

$$C_D = \frac{G_0}{\omega\sqrt{2}} \left(\sqrt{1 + \omega^2 \tau_p^2} - 1 \right)^{1/2} \tag{6}$$

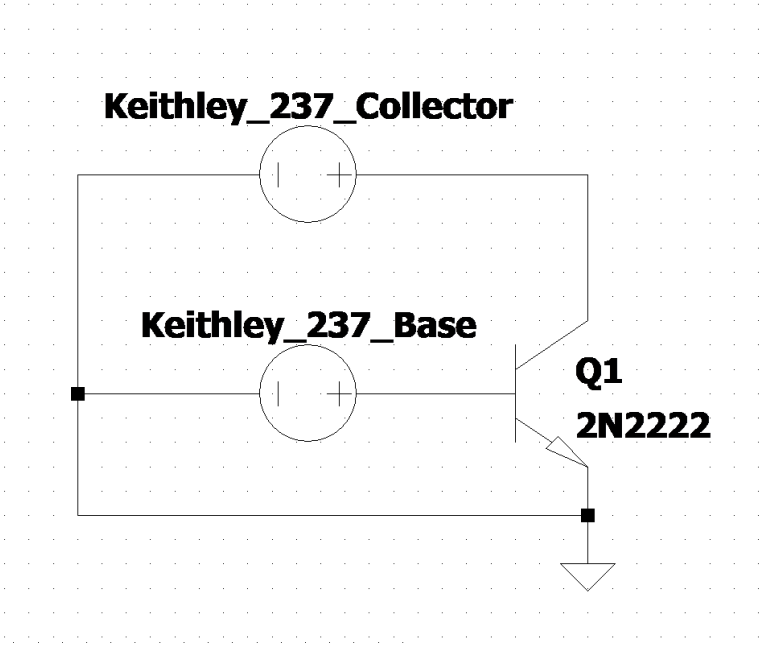

Figure 9: Circuit diagram for the current gain and gummel plot measurements. The Keithley 237 at the collector maintained 3.4 V and the Keithley 237 at the base swept from 0 to 1 V.

In Equation 6, G_0 represents conductance, ω is frequency of the signal, and τ_p is the lifetime of holes in the junction.

$$C_J = \frac{K_s \epsilon_0 A}{\left(\frac{(m+2)K_s\epsilon_0}{qb}(V_{Bi} - V_A)\right)^{1/(m+2)}} \tag{7}$$

In Equation 7, K_s is the dielectric constant, ε_0 is the permittivity of a vacuum, A is the area of the junction, m is the linearity of the junction, q is the electron charge, V_{BI} is the built-in voltage of the junction, and V_A is the applied voltage.

When voltage is applied to the contacts, V_A is much less than the V_{BI} of the junction, C_J dominates the capacitance of the device. As the V_A approaches V_{BI}, C_D becomes dominant and capacitance begins rising exponentially. From the CV, equations 6 and 7 can be fitted to the data, keeping A constant and thus, providing a calculation of the majority carrier lifetime.

3.2 Irradiations at the OSURR

Three transistors were irradiated at the OSURR using the rabbit facility. These transistors were irradiated to provide a baseline for expected damage at the NIF. 1 MeV(Si) fluence at NIF was expected to be $> 10^{12}$, so the OSURR irradiations are intended to bracket this this value to provide a baseline for expected changes to the devices.

Irradiations were accomplished at the OSURR on 29 January 2021. Transistors were irradiated individually. The reactor power, time irradiated, and resulting neutron fluence are listed in Table 1 These irradiations were meant to set expectations for circuit design and device performance and not sufficient for statistical damage analysis.

Table 1: Neutron exposures at OSURR based on reactor power and exposure time.

Power (kW)	Time (s)	Fluence (1 MeV(Si))
2	409	10^{12}
20	409	10^{13}
200	409	10^{14}

Unlike the NIF irradiations, OSURR devices were neither powered nor measured during irradiation. This was mostly due to reactor operation availability and the decision to use the rabbit tube facility [27]. This makes the test conditions different from those for the NIF irradiated transistors.

3.3 Experimental Circuit for NIF Irradiation

For the irradiations at the NIF, the transistors were operated in forward active mode during irradiation. Figure 10 provides the test circuit for NIF irradiations. Transistors being evaluated as devices under test (DUT) are labeled “DUT1” and “DUT2”. Resistors were placed at the collector and emitter of each DUT to convert

current to voltage drops using Ohm's Law, Equation 8, and in order to observe the time dependent shot dynamic changes with oscilloscopes [23]. A current source provided 20 µA of current to the base through a diode, used to block back flow of current during the shot. In order to remove current driven by ionizing radiation into the base of the DUT, a sacrificial transistor, labeled "SAC1" and "SAC2", was connected to the base of the DUT with the BE junction reverse biased in order to maintain a constant current at the base of the DUT during the irradiation [6].

$$I = \frac{V}{R} \tag{8}$$

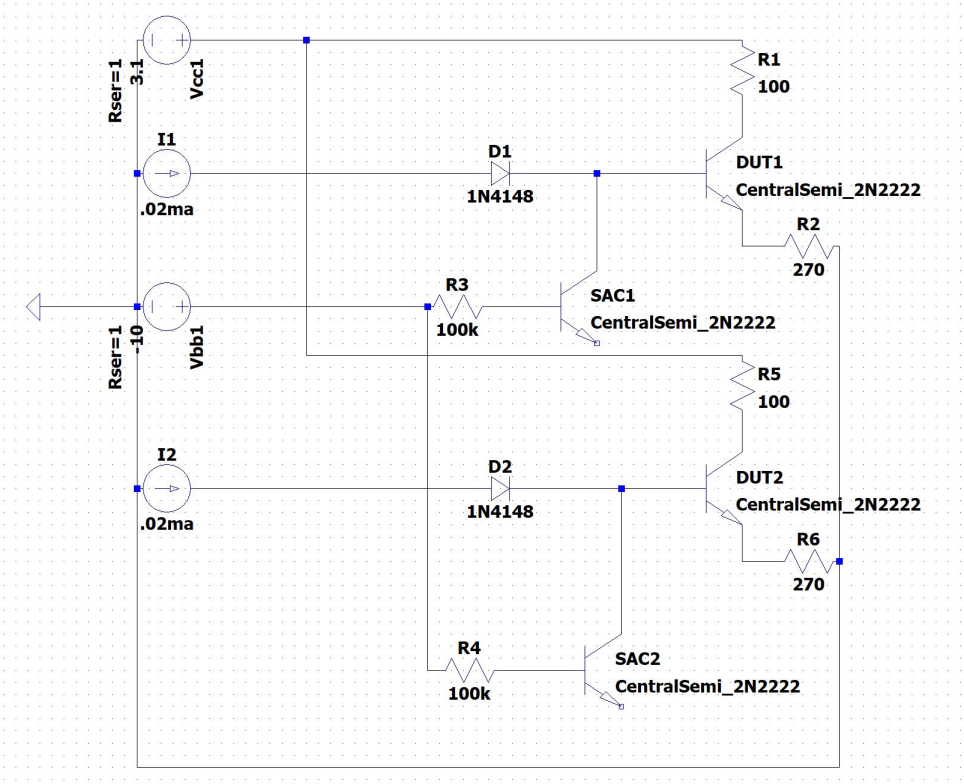

Figure 10: Circuit used at NIF for the ATHENA II experiment. The transistors being monitored are labeled DUT1 and DUT2. SAC1 and SAC2 are sacrificial transistors, included in the circuit to help maintain constant current at the base of the monitored transistors.

3.4 NIF Irradiation Experiment, shot N210526-001 with ATHENA II

Four transistors were irradiated at the NIF on 26 May 2021, shot N210526-001 with the ATHENA II apparatus. Two transistors were irradiated in each of the internal and external positions. During the shot, the transistors were connected such that there was 0.02 mA supplied to the base of each DUT and 3.1 V applied to collector of the transistors [6].

The NIF irradiation source required the use of a PDXP DT target energized with 1.2 MJ lasers. The PDXP released 10^{16} neutrons in 4π [26]. The ETA was set 60 mm away from the DT target. In the internal position, the devices were exposed to a 1 MeV(Si) equivalent neutron fluence of 1.09×10^{12} in 5 shakes. In the external position the devices were exposed to a 1 MeV(Si) neutron equivalent fluence of 1.06×10^{12} in 1 shake. The estimated uncertainty for these neutron fluences is 1-2% The fluence was measured with foil activation spectroscopy, and the timing profile was determined using MCNP models [1]. This is within the expectation of $> 10^{12}$ 1 MeV(Si) equivalent fluence. For comparison, the results in Chapter IV will use the 10^{12} 1 MeV(Si) equivalent fluence OSURR transistor alongside the NIF irradiated transistors.

To characterize the ionizing dose of the NIF irradiation, TLD-100 and TLD-400 chips were positioned in the internal and external positions. MCNP models were used to determine an estimated gamma dose prior to the shot. The measured ionizing dose for the internal devices was 3.5 times the modeled result. The external devices saw an estimated factor of 1.8 for the TLD-100 and 0.7 for the TLD-400. Table 2 summarizes the modeled and measured integral ionization dose for the TLD chips and silicon. There is a significant discrepancy, with multiple potential sources. Manufacturer error for the TLD chips is 15% for rad (TLD-100) and 30% for rad (TLD-400). Also, there is little data for inelastic neutron interactions with the materials inside ATHENA

[1]. As such, there is a discrepancy between the measured and modeled gamma data within the ETA.

During the shot, oscilloscopes were connected to monitor the potential at the collectors and emitters of the DUT. Two sets of dynamic data were obtained, a short scale 90 µs measurement and a longer 4.5 s measurement. The short scale was measured at 16 GSa/s. The long scale measurement was made at a rate of 40 MSa/s.

Table 2: ATHENA irradiation position neutron environment metrics for a 10^{16} neutron shot yield [1].

Position	TLD / Si	Modeled rads(TLD/Si)			Measured rads(TLD/Si)
		Inelastic and Delayed	Source X-rays[1]	Total	
Internal	100	382 ± 1%	0	382 ± 1%	1,364 ± 8.7%
	400	386 ± 1%	0	386 ± 1%	1,289 ± 14.9%
	Si	169 ± 1%	0	169 ± 1%	N/A
External	100	88 ± 4%	249 ± 4%	337 ± 1%	618 ± 11.5%
	400	96 ± 4%	886 ± 2%	982 ± 2%	672 ± 7.9%
	Si	98 ± 1%	0	98 ± 1%	N/A

[1]Estimated upper-bound based on NIF x-ray survey spectrometer

3.5 Post Irradiation Measurements

Following recovery of the transistors, they were extracted from the circuit boards and remeasured as with precharacterization. Statistical analyses were made on I_{BC} characteristics for comparison. Gain measurements were processed and calculations were made for the inverse gain degradation.

3.6 Device Simulations using DEVSIM

In order to evaluate parameters affecting transistor behavior following irradiation, DEVSIM, an open source technology computer-aided design (TCAD) software focused on semiconductor device simulation, was used. Included in DEVSIM are

meshing tools and partial differential equation solvers that can be used to simulate semiconductor device performance. The software calculates carrier statistics and fields based upon the carrier and continuity equation solutions discretized to a device mesh. DEVSIM solves a self consistent matrix solution using the boundary conditions set by bias conditions at the device boundaries (i.e. contacts) [28]. Equations are included to calculate features such as carrier density, current, and electric field throughout the device based upon device doping, materials, and geometric structure.

To simulate a BJT, doping of each region was estimated (Table 3). Using these doping concentrations, depletion widths were calculated for each junction in the device based upon IV measurements. These calculations proved the most carrier depletion into any region was assured to be 0.882 µm into the collector (see Appendix **??**). The discrete BJT dimensions are listed in Table 4. The mesh was configured to be more dense at the pn junctions, and refined afterward based upon the change in electric field. The 0 V bias solution with doping profile is shown in Figure 11.

Table 3: Initial doping characteristics for simulation model

Region	Doping Concentration
Emitter	10^{18} cm^{-2}
Base	10^{16} cm^{-2}
Collector	10^{15} cm^{-2}

Table 4: Initial region dimensions for the simulation model

Region	Width	Depth
Emitter	5 µm	4 µm
Base	10 µm	2 µm
Collector	10 µm	25 µm

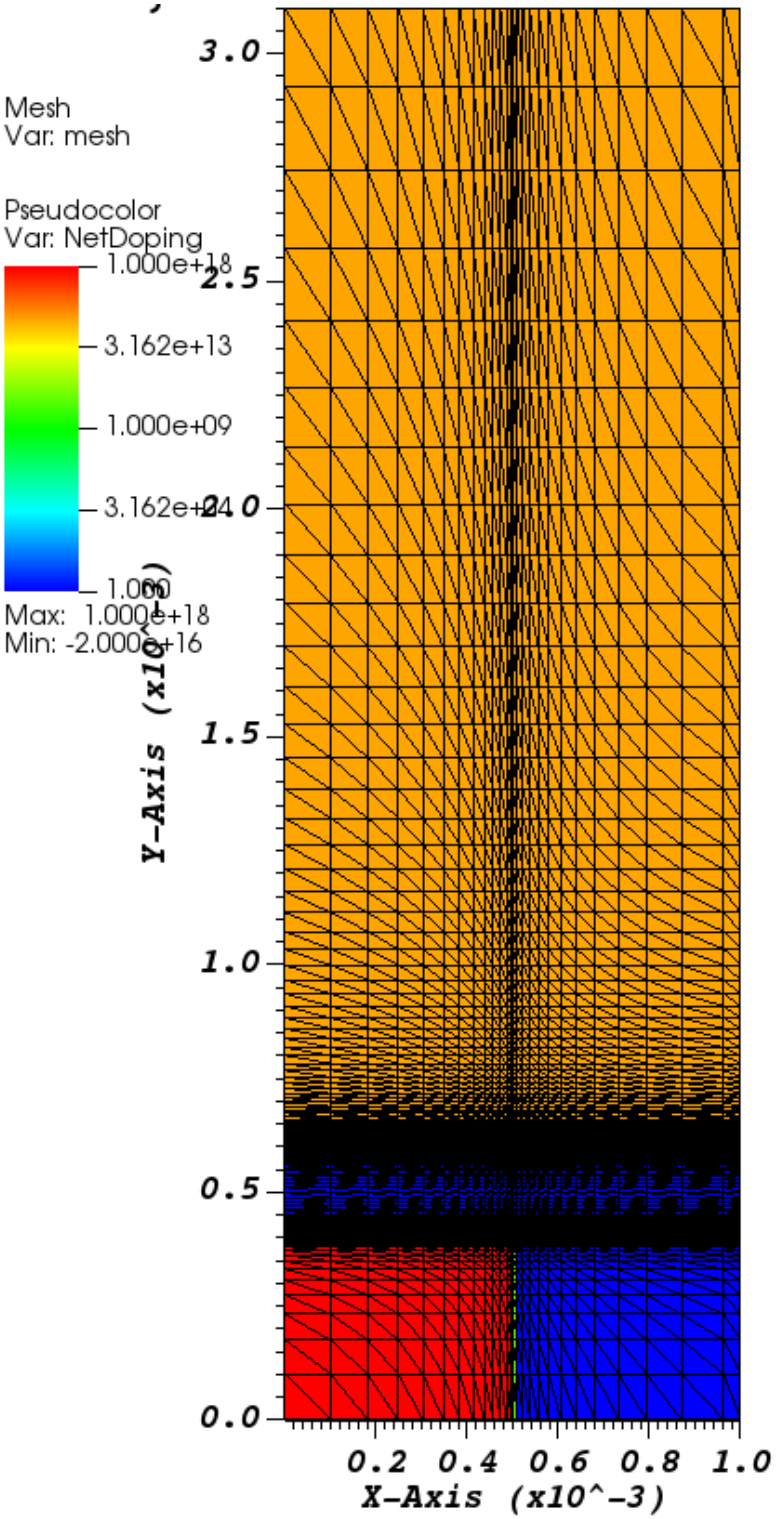

Figure 11: DEVSIM simulation grid showing the net doping for each region.

DEVSIM was used to evaluate how parameters affect the BJT gain following irradiation. External Python programs were written to evaluate bias ramping to 3.4 V on the collector, then ramped the base voltage from 0 to 1 V, recording the current values at each contact every 0.01 V. Results are discussed in Chapter IV and code can be found in Appendix C.

IV. Results and Analysis

4.1 Lifetime Analysis

The majority carrier lifetime was calculated using the CV measurements following irradiation. Figure 12 shows the CV measurement across the base-collector junction of the 2N2222 transistors before and after exposure to each neutron environment. Also included is an unirradiated device for comparison. The minority carrier lifetime (τ) was calculated by fitting the equations 6 and 7 using a Newton-Method solver and extracting the lifetime.

Although not conclusive, the results (Table 5) are encouraging as the extracted lifetime for each device except the NIF external are the same, indicating that the damage for the same fluence is the same, and essentially immeasurable. However, for the NIF external, the higher energy spectrum provides a 50% reduction in lifetime. These results are definitely worthy of further attention in subsequent experiments. More data is required to resolve this and confirm that the change in lifetime observed in Figure 12 is valid.

Table 5: Lifetime (τ), linearity of junction (m), built-in voltage (V_{bi}), area of junction (A), and effective carrier concentration (β) for the selected transistors.

Transistor	τ	m	V_{bi}	A	β
Unirradiated	7×10^{-7}	1.00	0.5	4.51×10^{-5}	1.5×10^{19}
OSURR 10^{12} 1 MeV(Si)	7×10^{-7}	0.85	0.5	4.51×10^{-5}	4.6×10^{18}
NIF Internal	7×10^{-7}	0.85	0.55	4.51×10^{-5}	4.6×10^{18}
NIF External	3×10^{-7}	1.4	0.53	4.51×10^{-5}	5.5×10^{20}

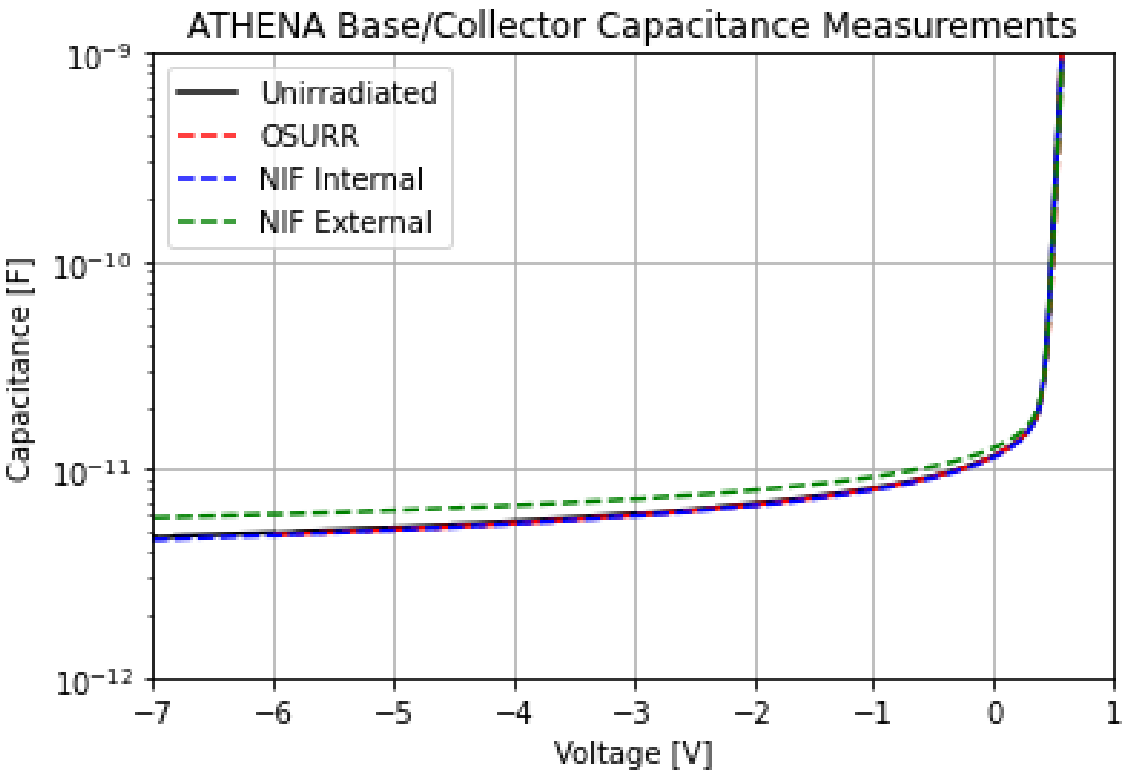

Figure 12: Lifetime analysis of irradiated transistors. 2N2222 transistors primarily follow the lowest line on the plot, with the decreased lifetime in the NIF external transistor increasing its capacitance above that of the others in reverse bias.

4.2 Current-Voltage (I_{BC}) Post irradiation Measurements

The I_{BC} measurements characterize the junction in its steady state operation under direct current. Measurements were obtained using a voltage sweep from -8 to 1 V, in 5 mV increments, applied between the base and collector of the transistor. The emitter was connected to a physical ground for all of these measurements. Using this measurement, changes to leakage currents, carrier mobility, and carrier lifetime can be observed while the junction is in reverse bias. The inflection point, where I_{BC} changes from negative to positive is also an indication of accumulation of junction space charge buildup on defects.

4.2.1 2N2222 Pre-Irradiated IV Characteristics

To ensure the uniformity of the 2N2222 transistors, 16 unirradiated transistor I_{BC} measurements were obtained. Plotted in figure 13, the unirradiated transistor I_{BC} are indistinguishable from each other. The transistors reach breakdown when $V_A < -7$ V, above which the standard deviation between transistors at a given voltage is ∼nanoamps. The figure does not include error bars, due to the dominant error (machine error) being less than 0.04% of the magnitude of the current.

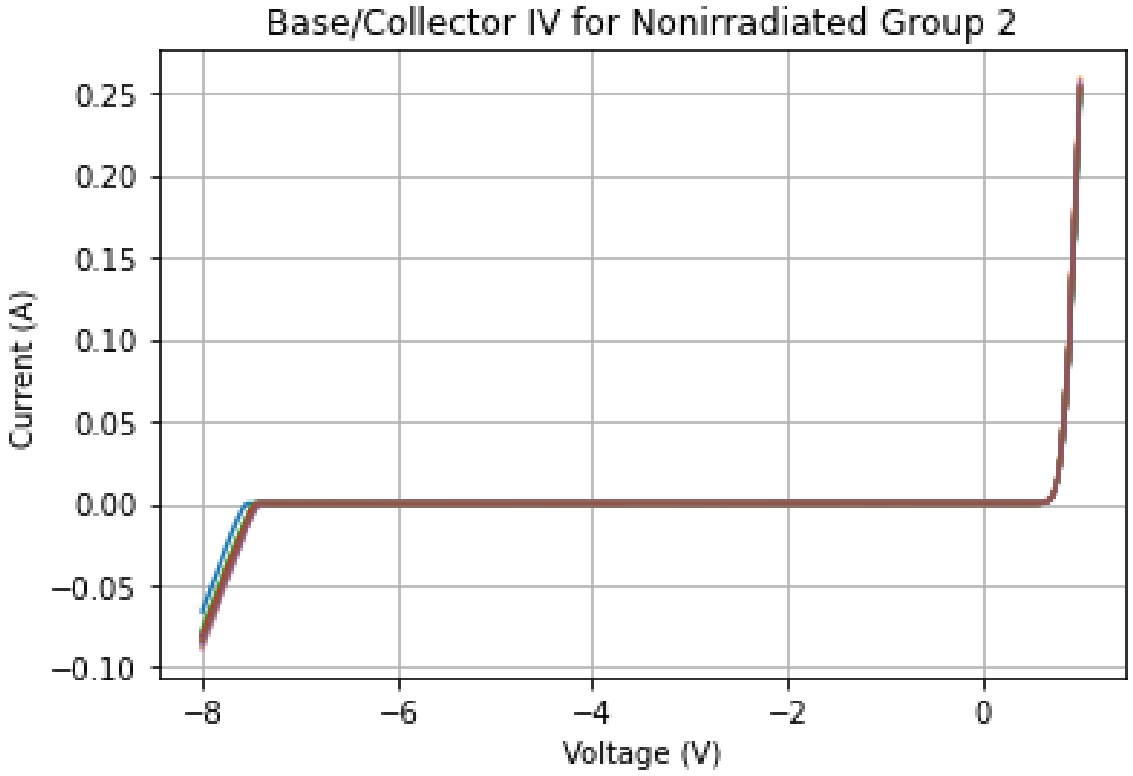

Figure 13: The I_{BC} measurements for 16 unirradiated transistors are statistically inseparable from each other.

Using Kruskal-Wallis statistics, the p-value was calculated across all unirradiated transistors for the entire voltage range. With a p-value of 0.999, there is at least a 95% confidence that the distribution of current over the measured voltage range is the same for all 16 transistors. The unirradiated 2N2222 transistors are statistically inseparable. Therefore, only one unirradiated device measurement was used in the remaining comparisons in this research.

Table 6: Kruskal Wallis statistic p-values for each group of transistors: a set of 16 unirradiated transistors, the OSURR irradiated transistors, and the transistors sharing approximately 10^{12} 1 MeV(Si) fluence.

Transistors in statistical group				p-value
16 unirradiated 2N2222 BJTs				0.999
Unirradiated	10^{12} 1 MeV(Si)	10^{13} 1 MeV(Si)	10^{14} 1 MeV(Si)	1.43×10^{-62}
Unirradiated	10^{12} 1 MeV(Si)	ATHENA Internal	ATHENA External	0.368

4.2.2 Characteristics of Devices Irradiated at OSURR

The IV measurements for each OSURR irradiation is shown in Figure 14 along with an unirradiated for comparison. Evident in the IV characteristics is the increased recombination leakage in the reverse bias With increasing total neutron fluence. Also, there is no change to the current inflection point, removing any expectation of trapped charges forming in the junction region.

In the statistical analysis of I_{BC}, the Kruskal-Wallis p-value on table 6, provides a numerical representation of the difference between transistors. At a value of only 1.43×10^{-62}, or essentially 0, it is much lower than the statistical confidence value for $\alpha = 0.05$. Therefore the IV relationships are separable, and the OSURR irradiations have resulted in statistically different IV characteristics.

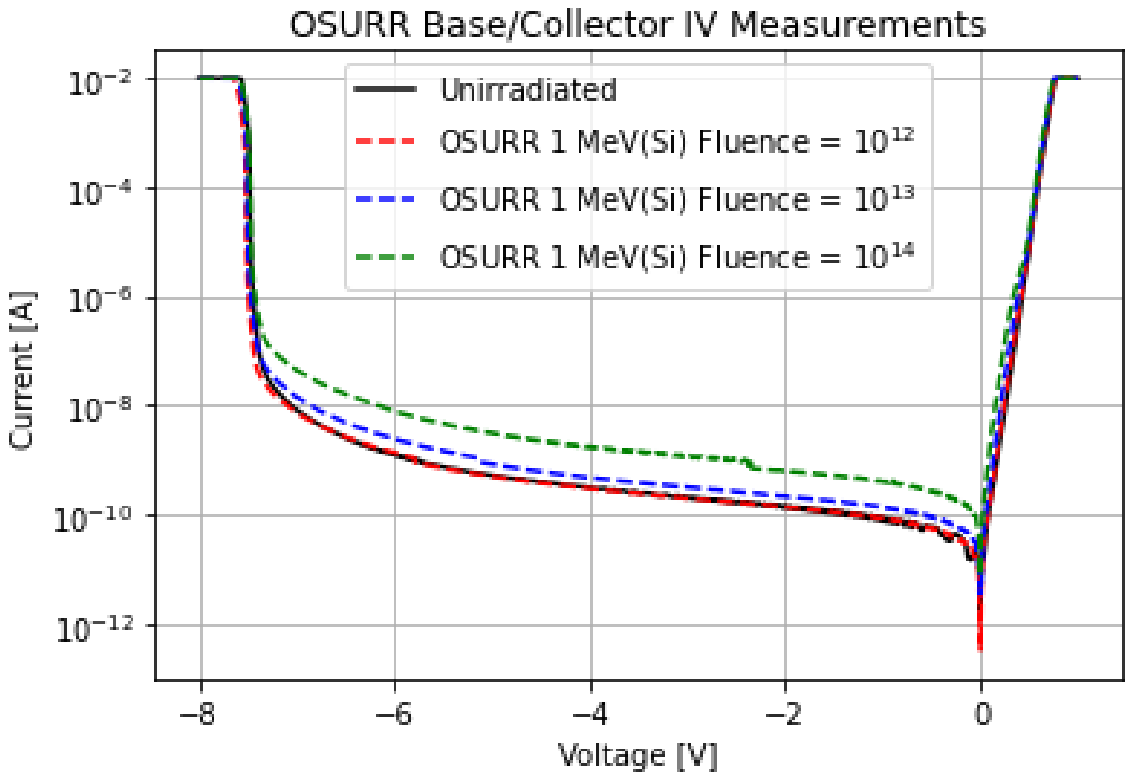

Figure 14: Base-Collector IV Measurements from transistors irradiated at OSURR. The leakage current as the BC junction operates in reverse bias has a statistically significant rise as the magnitude of fluence on the transistors is increased.

4.2.3 Analysis of Transistors from the ATHENA II Experiment

Four transistors were irradiated at NIF, two internal and two external. When being extracted from the circuit board the pins for one internal and one external transistor were cut too short to make reliable measurements, reducing the sample set to one. As such, all NIF results are based upon one transistor in each environment.

Figure 15 presents the I_{BC} relationships for irradiated transistors. An unirradiated transistor is presented for the baseline and the OSURR transistor irradiated at an ∼equivalent 1 MeV(Si) fluence for comparison. The IV relationships are nearly indistinguishable.

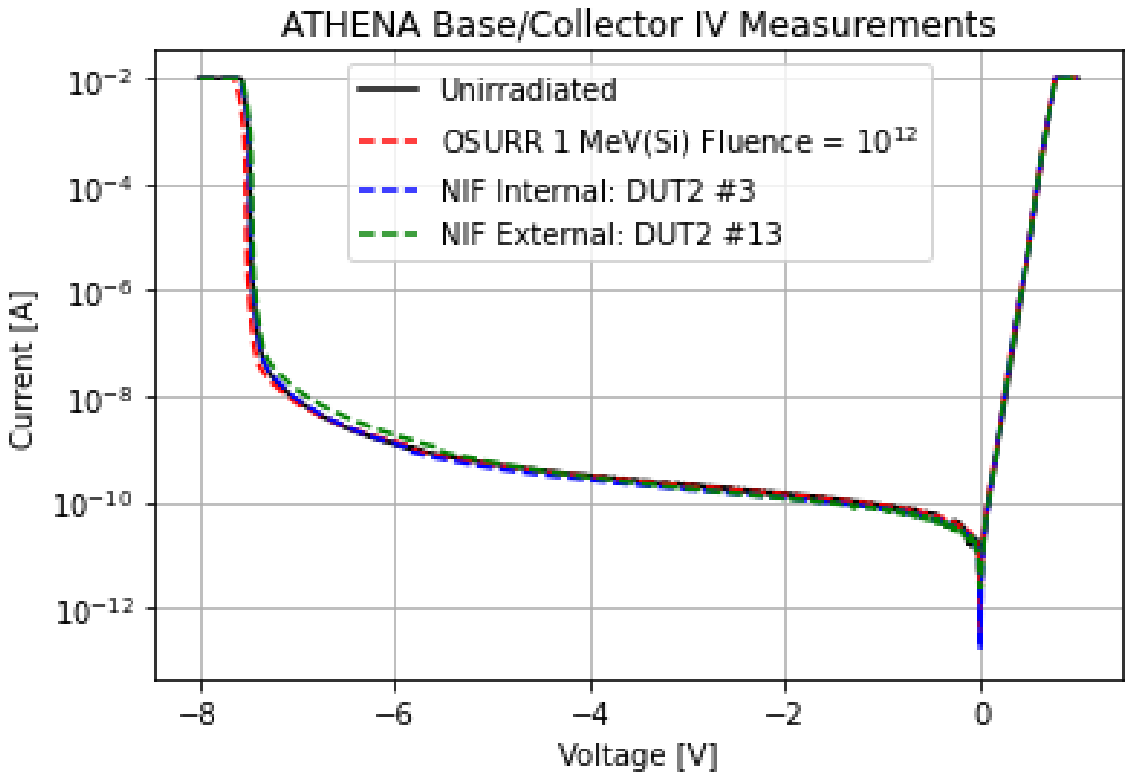

Figure 15: Base-Collector IV Measurements following pulsed irradiation at the NIF. "Internal" and "External" refer to their location on the ETA which were exposed to different neutron spectra. The OSURR transistor is included to provide insight into whether the short pulsed environment affects the BC junction operation differently than the steady-state reactor environment.

Table 6 provides the results of the Kruskal-Wallis analysis of the devices irradiated to 10^{12} fluence and one unirradiated device. The p-value is above the $\alpha = 0.05$ threshold, meaning these devices are statistically performing the same.

4.3 Post Irradiation Gain Degradation Analysis

The calculation of forward active current gain (β) uses the currents measured at the collector and base contacts [22]. When making these measurements shown, in Figure 16, the relationship between I_c and I_b can be determined. In an ideal BJT, the Gummel plot should have a nearly parallel I_c and I_b characteristic. However,

in practice, junction doping is not homogeneous leading to variations in available carriers. Thus the Gummel plots, and gain parameters have features that cannot be replicated easily. Added details related to the Gummel plots for all measured transistors can be found in Appendix A. Aside from these variations, the Gummel plots can be used to analyze the gain degradation.

Figure 16 shows the Gummel plot relating I_c, I_b, and β. There is a slight overlap immediately after I_b becomes positive and each current curve becomes linear during saturation of the regions of the transistor. The instrument connected to the collector reaches compliance at 0.1 A.

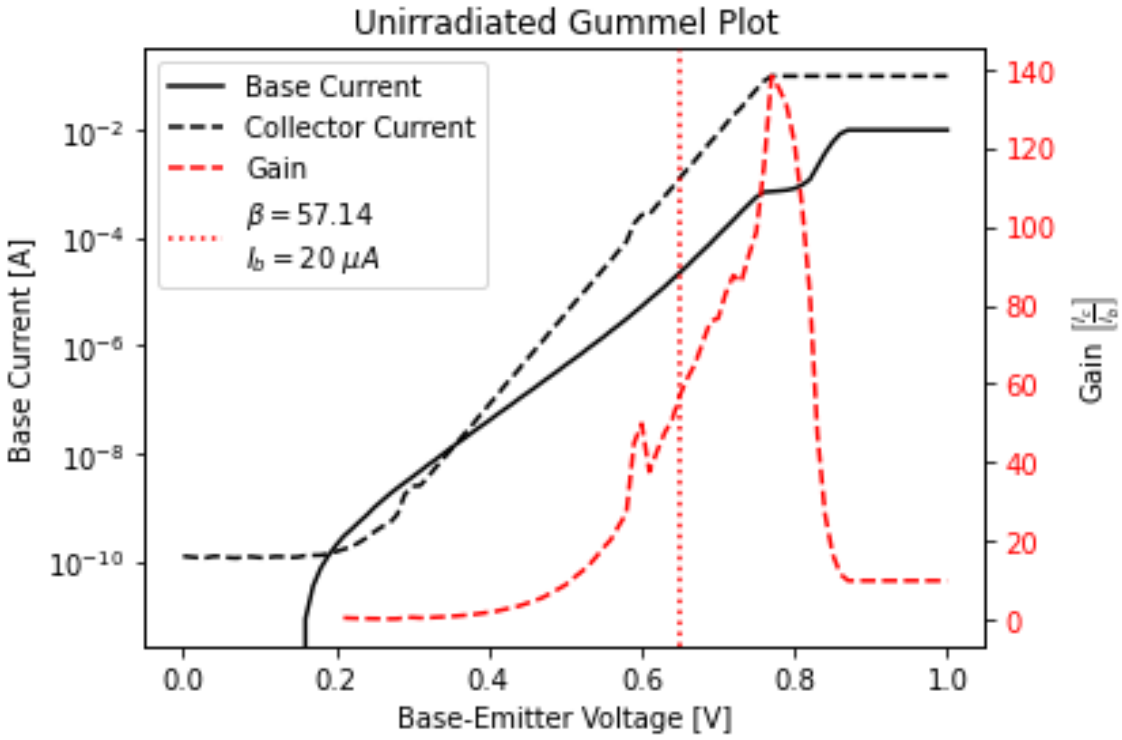

Figure 16: Unirradiated transistor Gummel plot with the relationship between collector and base currents and the current gain of the transistor.

4.3.1 Ohio State University Research Reactor Irradiation Results

Post irradiation inverse gain degradation results from the OSURR transistors produced mixed results, as shown in Figure 17. As the total neutron fluence increases, the gain is expected to decrease, due to reduced mobility and lifetime. Although this is generally true, the gain at a fluence of 10^{12} is an anomaly, expected to be above 16.24 and below 57.14, more in line with the values for the NIF. In Figure 16 the unirradiated transistor has a maximum gain of around 140. For a fluence of 10^{14} the gain reaches only 20 at its maximum. The inverse gain degradation at that fluence is two orders of magnitude greater than the degradation when fluence is only equal to 10^{12}.

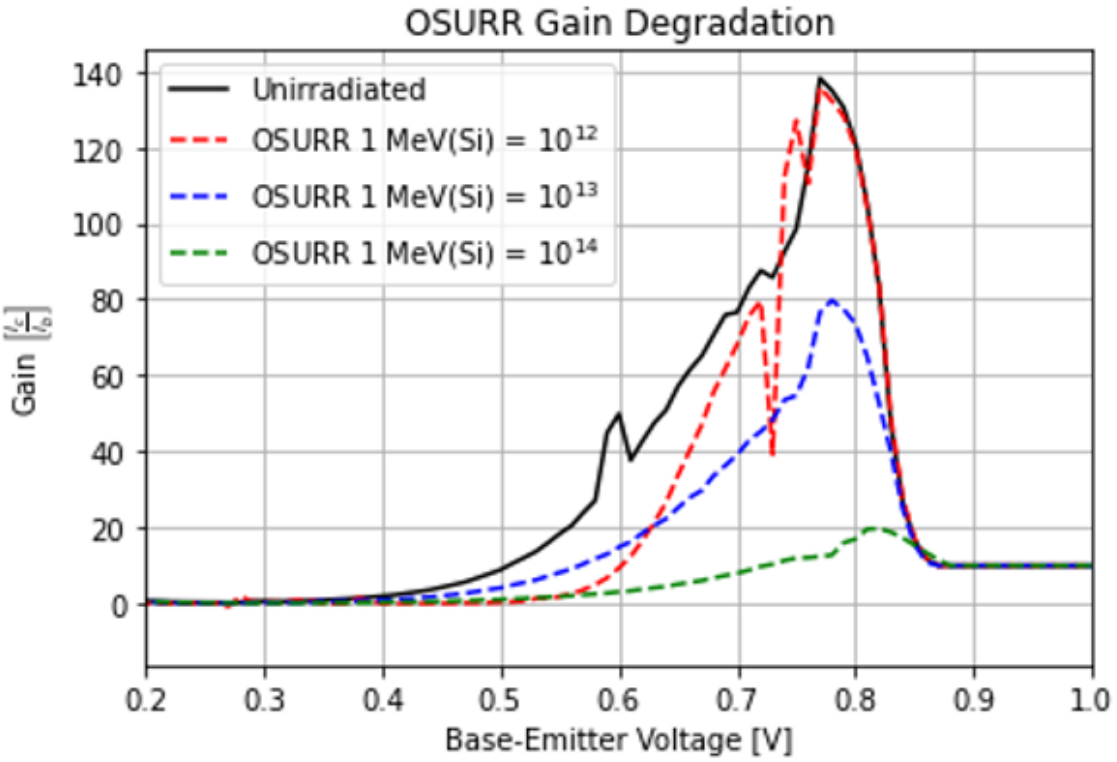

Figure 17: This plot clearly displays the reduction in current gain as irradiation affects the transistors. As the magnitude of fluence is increased, the maximum gain achieved is significantly reduced from nearly 140 to about 20.

4.3.2 Gain Analysis of Devices Irradiated by NIF in ATHENA II

Each irradiation at the NIF provided a neutrons fluence of $\sim 10^{12}$ 1 MeV(Si) equivalent, regardless of location. The gain for this fluence is consistent with the expectation to be above 16.24 and below 57.14. The gain plots are shown in Figure 18. The inverse gain degradation is very small in each case, on the order of 10^{-3} or less, consistent with observations of the IV relationships and lifetime measurements.

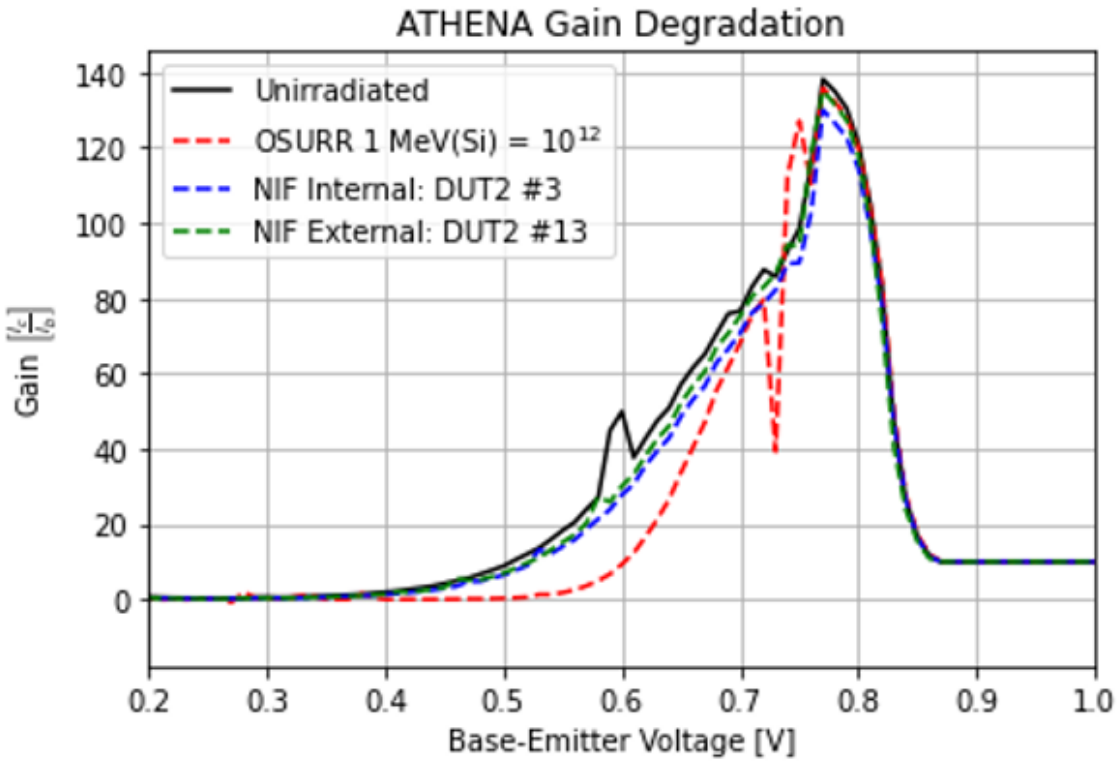

Figure 18: All transistors' gain follows the same trend, with little clear gain reduction.

Table 7: Gain measured for each transistor and DEVSIM simulation when collector current equals 20 microamps and inverse gain degradation

Transisitor	**Gain at $I_b = 20\mu A$**	**Inverse Gain Degradation**
Unirradiated	57.14	-
OSURR 1 MeV(Si) Fluence = 10^{12}	9.346	0.08950
OSURR 1 MeV(Si) Fluence = 10^{13}	16.24	0.04406
OSURR 1 MeV(Si) Fluence = 10^{14}	2.0388	0.4730
NIF Internal	42.94	0.005789
NIF External	46.15	0.004169

4.4 Dynamic Measurements during ATHENA II

Oscilloscopes connected to the circuits during the NIF irradiation collected voltage during the course of the irradiation. One oscilloscope measured the internal transistors for 90 µs. Another measured for 4.5 s. Two more oscilloscopes measured the external transistors for the same times. The resistors placed in the circuit allows for conversion from voltage to current using Ohm's law.

Figure 19 and 20 presents the current for 90 µs after the shot at the collector of the internal and external transistors. There is an initial off scale oscillation for the first ∼10 µs. After this time, the current is reduced to approximately 4 mA. Both transistors in each environment performed in nearly the exact way, providing confidence in the measurements and the response.

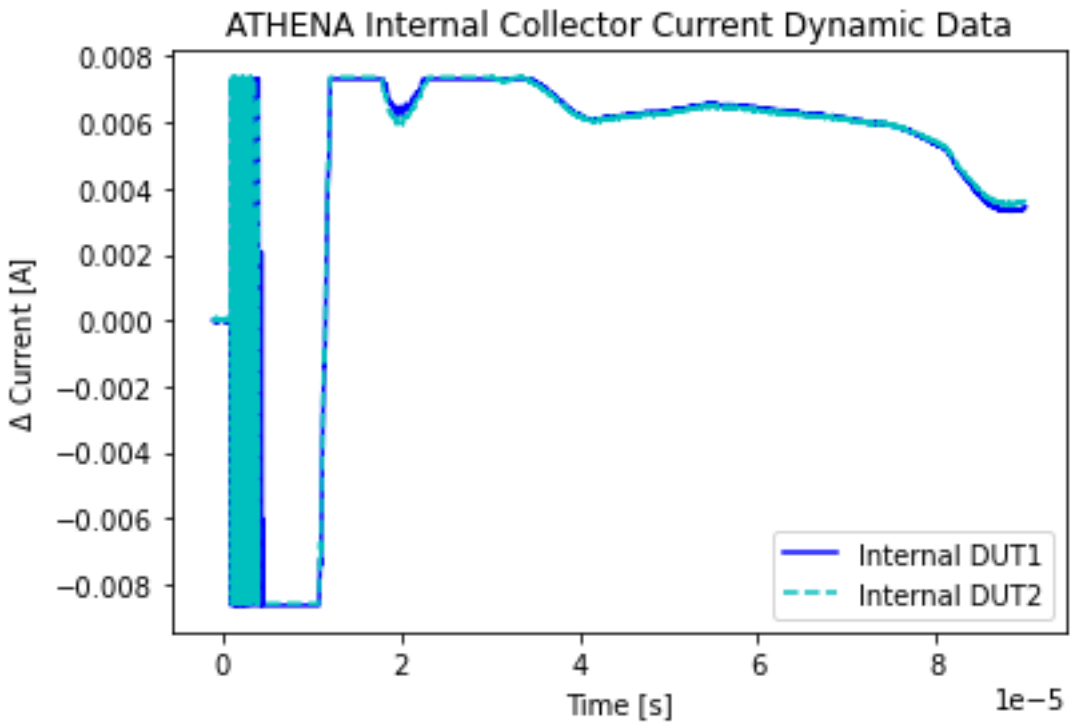

Figure 19: Change in collector current over time during the ATHENA NIF shot for the transistors internal to the ETA.

There is a measurable difference in response between the internal and external transistors. In figure 19, the internal devices return to 4 mA near 80 µs, but in figure 20, the external devices are nearly stable at 4 mA at ∼40 µs after the pulse. Because each set of transistors is exposed to a different neutron spectrum, the results imply that the difference in neutron spectrum produces different initial damage.

The dynamic data from the 4.5 s time scale was unusable due to improper oscilloscope settings. Figure 21 presents the change in collector current obtained from the oscilloscope set to measure for 4.5 s. This figure shows the data truncated to the first 90 µs to compare the features between the long and short recordings. The 4.5 s oscilloscope recorded only the initial irradiation burst, the remaining features that could be observed in Figure 19 are off scale in Figure 21.

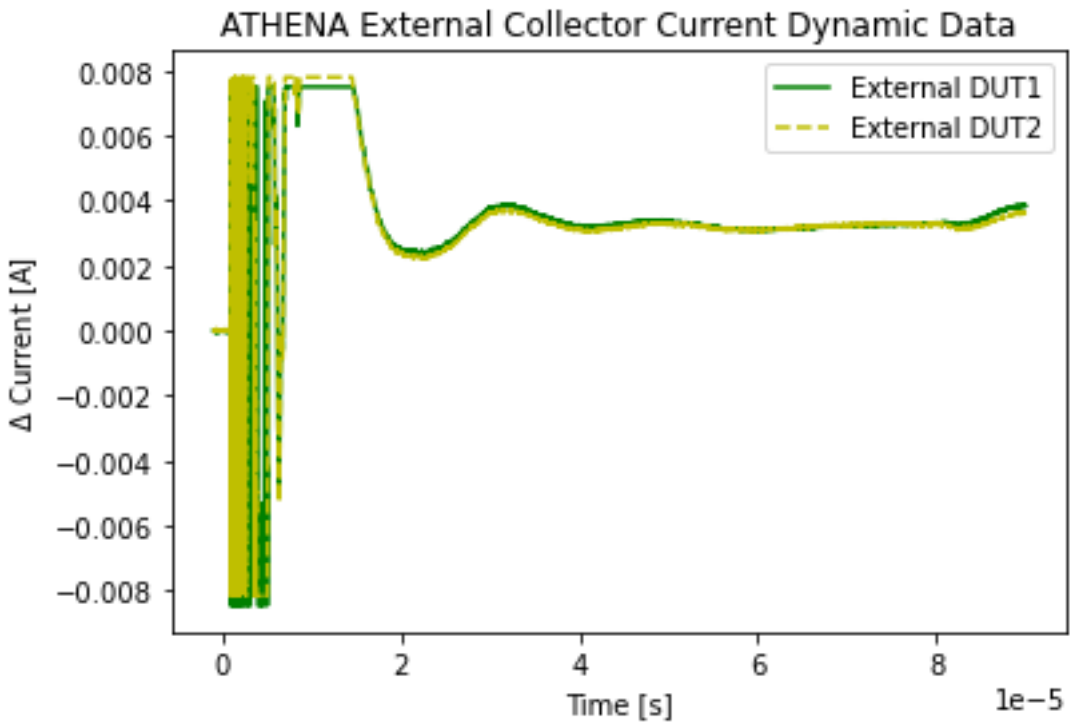

Figure 20: Change in collector current over time during the ATHENA NIF shot for the transistors external to the ETA.

In order to improve dynamic data collection, the current data can be used to produce a new voltage range for the oscilloscopes. The dynamic data suggests that most of the features of interest are above the initial voltage of the collector. The oscilloscope could be set with a range such that the lower limit is ∼200 mV below the initial voltage and the upper limit, 1.5 V above the lower limit. Based on the response from ATHENA II, this should capture most of the response curve for the collector. To make up for the inconsistency between DUT measurements, the same settings should be ensured for each DUT in an environment.

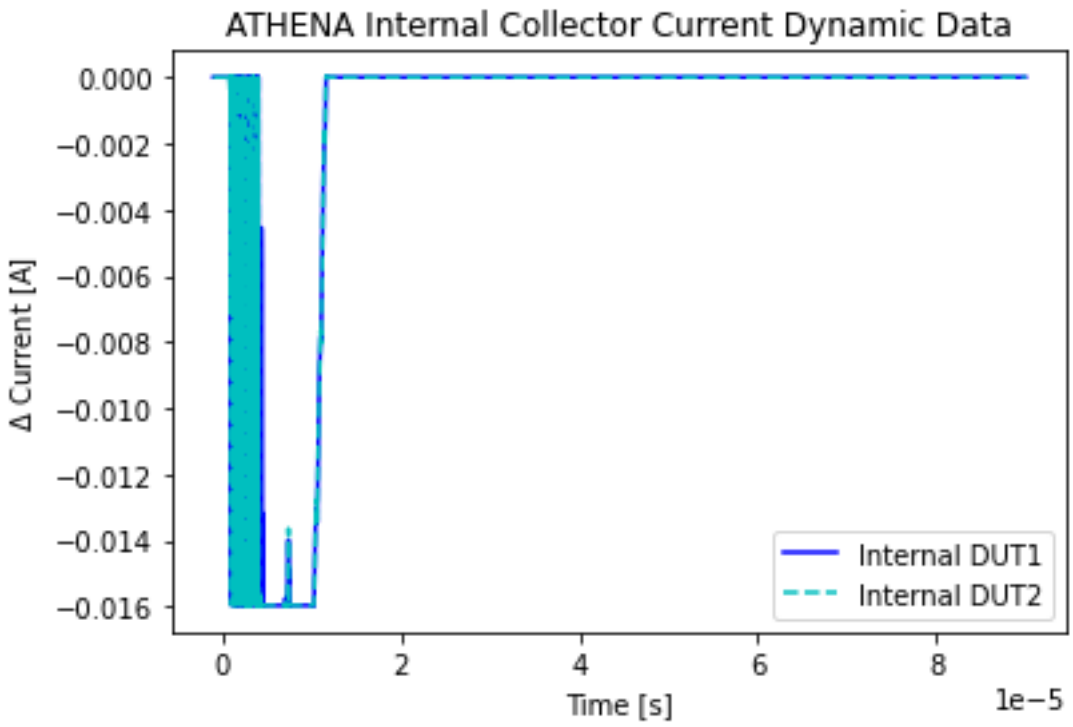

Figure 21: Change in collector current over time during ATHENA NIF shot for transistors internal to the ETA using the 4.5 s reading oscilloscope. This data is truncated to 90 µs to compare with Figure 19.

4.5 Gain Analysis Using DEVSIM Device Analysis Program

Without sufficient knowledge of important BJT transistor design beforehand, an acceptable simulation of the 2N2222 transistor performance could not be modeled. However, the simulation model was useful for exploring the effects of changes to device parameters within the simulation that affect the measurable device performance. DEVSIM was used in conjunction with the Gummel plots and gain calculations to explore how radiation induced changes to lifetime and mobility affect gain.

Using DEVSIM to simulate currents used to produce the Gummel plots, resulted in similar IV relationships to the measured currents, with several key differences;

- The slope of I_b and I_c are more parallel in the simulation,
- The magnitude of I_b and I_c is reduced in the simulation,

- The IV behavior differs when $V_b > 0.8$ V,
- There is significantly lower current gain during the voltage sweep.

To compare the simulation with the experimental data, the gain is measured for the base current equal to 20 µA. If the DEVSIM simulation was accurate, the gain would match the unirradiated transistor at a base current equal to 20 µA. Thus, after many parametric adjustments, a qualitative analysis was used.

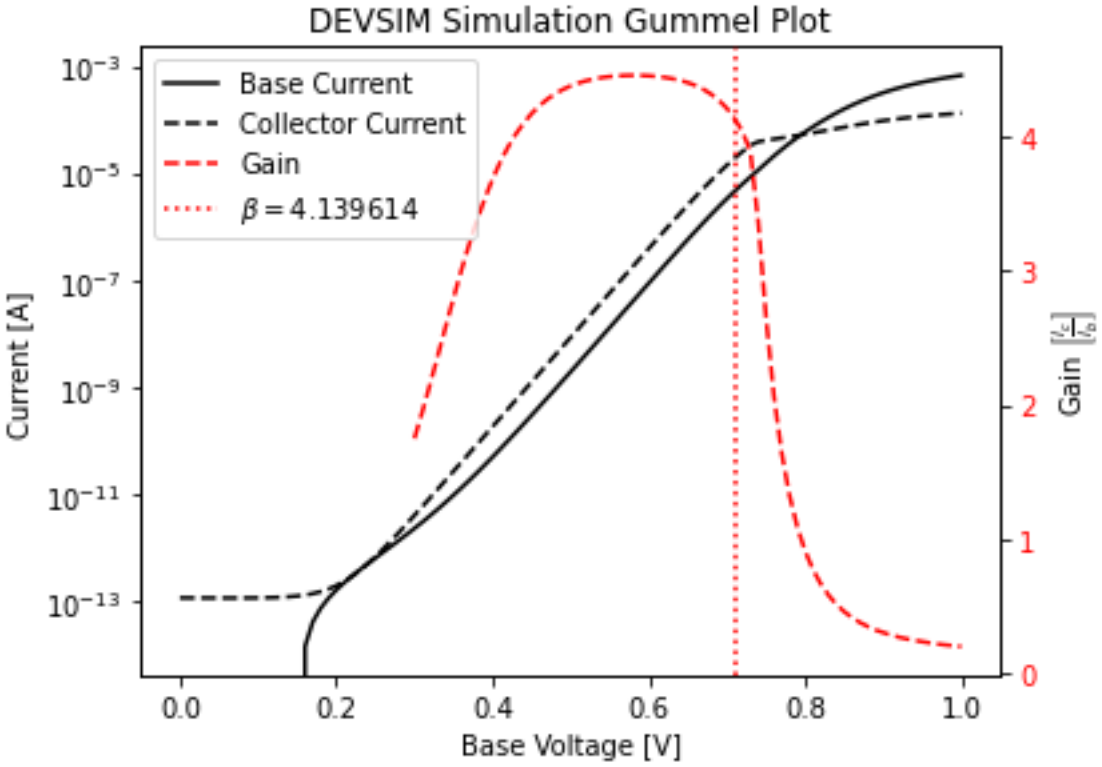

Figure 22: Gummel plot for DEVSIM simulated BJT. Base and collector current shows similar behavior to experimental transistors, but at a lower magnitude. Significantly lower gain is shown during the sweep, as well.

Because neutron irradiation affects carrier lifetime and mobility, the Gummel simulation was conducted using variations in carrier lifetime and mobility. Based upon Sze [22], electron mobility has practical limits between 400 and 1200 cm^2/V-s and lifetimes between 10^{-5} and 10^{-9} s. Table 8 presents the effect of lifetime and

mobility on the simulated gain. Based upon the DEVSIM simulation, changes to lifetime within practical limits has no observable effect on the transistor gain. Changes to the mobility within the practical limits of 1200 to 800 cm^2/V-s, reduced the gain by 1.6%. At the lower practical limit of of 100 cm^2/V-s, the gain is reduced by 93% from the original to 0.30 cm^2/V-s.

Figure 23 shows the decrease in gain as the electron mobility is reduced. The base current reaches 20 µA at a higher B-E voltage. The gain reduction is less, in all simulations, than the 96% between the unirradiated and 10^{14} 1 MeV(Si) irradiated transistors.

Table 8: Gain of DEVSIM transistor with changes of lifetime and mobility

Lifetime (s)	Mobility (cm^2/V-s)	Gain (at I_b = µA)
10^{-6}	1200	4.40
10^{-6}	800	4.33
10^{-6}	400	4.13
10^{-6}	100	0.30
10^{-7}	1200	4.40
10^{-7}	800	4.33
10^{-7}	400	4.13
10^{-7}	100	0.30
10^{-8}	1200	4.40
10^{-8}	800	4.33
10^{-8}	400	4.13
10^{-8}	100	0.30
10^{-9}	1200	4.40
10^{-9}	800	4.33
10^{-9}	400	4.13
10^{-9}	100	0.30

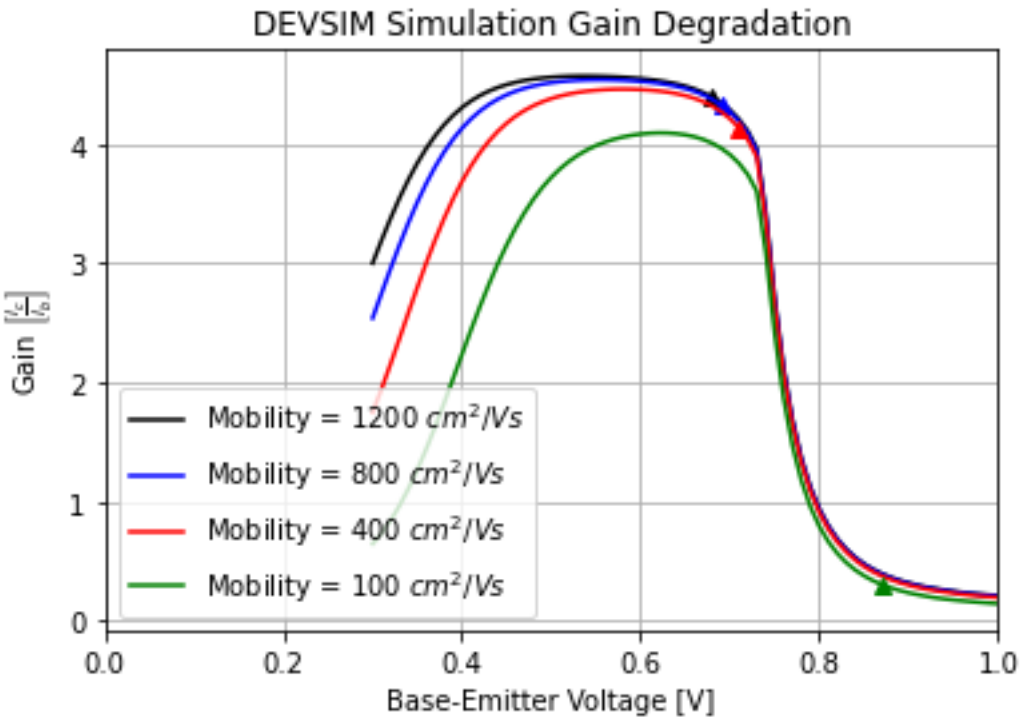

Figure 23: Gain degradation as mobility is changed in DEVSIM simulation. As mobility decreases the gain amplitude decreases. Triangles indicate the point where the base current reaches 20 µA.

V. Conclusions

This research provides evidence that regardless of neutron spectrum source, the late term performance effects on silicon bipolar junction transistors is similar, when accounting for the NIEL difference via the 1 MeV(Si) equivalent fluence. Using alternating current measurements, such as during the C_{BC} measurement, lifetime differences suggest that the neutron spectrum produces different primary damage species and this difference affects the dynamic current. The later steady-state measurements, such as the I_{BC} measurement, result in no difference. This means that the final, permanent defects are primarily the same and have the same effect on performance.

The internal and external transistors responded differently following a neutron pulse, at least in the first 90 µs after the pulse. The evolution of the current, and thus the damage species recovered over time. Although the long term measurements were not used due to incorrect oscilloscope settings, the recovery in the short term data was promising. The temporal evolution of the response could indicate a difference in defects created by the different spectra being received.

DEVSIM provides an open source tool for modeling semiconductor devices, but presently, without knowing the exact dimensions of the 2N2222 transistors, modeling exact specifications for this experiment is not possible. With more parametric experimentation with the software, testing other physical dimensions, doping levels, and doping gradients, a more accurate representation of the devices could be created. An issue with DEVSIM is a lack of resources and documentation on its use outside of the published manual. With more work using the software, documentation and tutorials can be improved.

ATHENA II provides progress towards recreating the TN+PFS spectrum for analyzing the effects of that pulsed spectrum on electronics in its inner cavity. Between the dynamic behavior of the transistors during irradiation and the C_{BC} measurement,

a difference in operation can be observed between devices irradiated in either neutron environment created during the NIF irradiation pulse. Larger neutron fluences are required to achieve relevant fluences for nation security needs.

5.1 Future Work

There are several tasks that can be put in to future work in this area of research.

It is important to improve statistical analyses by increasing the sample size of irradiated transistors. Not considered in this research, was the effect of gamma rays during irradiation, but capturing gamma irradiation data is important for the complete characterization of the radiation environment. Improvements to neutron yield in the NIF are also important to meeting national security relevance.

The "airbox" behind the ATHENA platform contains space that can be used for placement of more transistors [29]. These would not receive the same spectrum as those placed in the interior cavity, but the spectrum can be measured and total fluence calculated using additional foil packets. Additional irradiated transistors would improve the statistical significance of ATHENA.

A concern with the ATHENA platform is gamma production within the materials of the ETA. In modelling work for ATHENA II, the gamma production was thought to have be low [1]. Gamma characterization is important as it contributes ionizing radiation to the microelectronics being observed and affects the dynamic data being collected [29]. Dynamically capturing gamma pulse data during the shot is important to accurately represent the complete radiation environment being provided by the NIF and the ATHENA platform.

Since the ATHENA II shot at NIF, NIF has increased the source efficiency with the Hybrid E target [29, 30]. Much could be achieved in replicating shot N210526-001 at the higher total fluence and repeating all measurements, but with a fluence

above 10^{13} 1 MeV(Si). Based on measurements of the OSURR transistors, this would provide measurable damage via IV and gain degradation that would serve to answer the primary hypothesis of this research.

Including this as future research is important to meeting the needs of the radiation effects community. With every iteration, the ATHENA platform improves. The NIF in conjunction with ATHENA will build toward meeting requirements for testing in a relevant environment for TN+PFS and provides proof of concept for potentially creating other relevant neutron environments.

Appendix A. Additional Gummel Plots

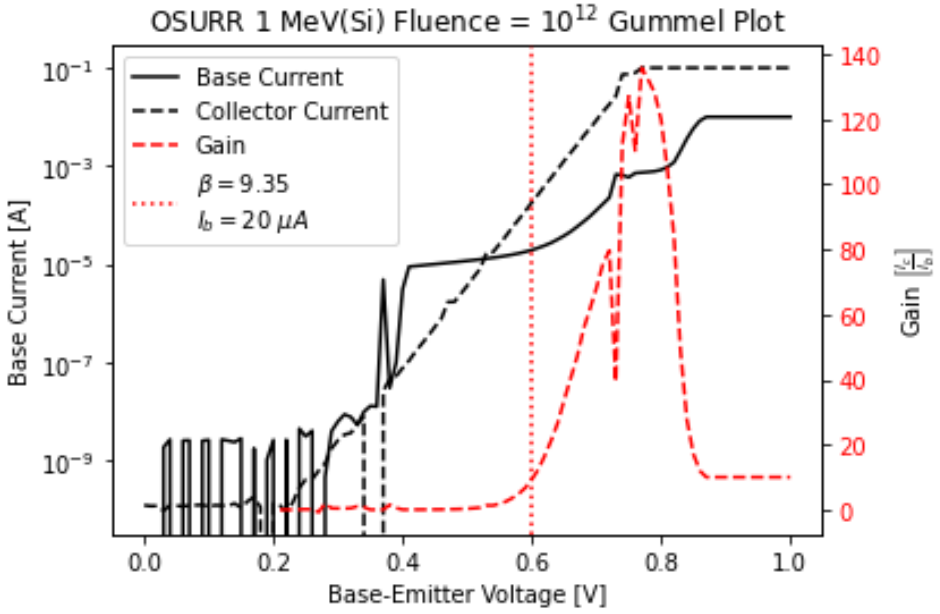

Figure 24: Gummel plot for the OSURR transistor irradiated at 10^{12} 1 MeV equivalent fluence.

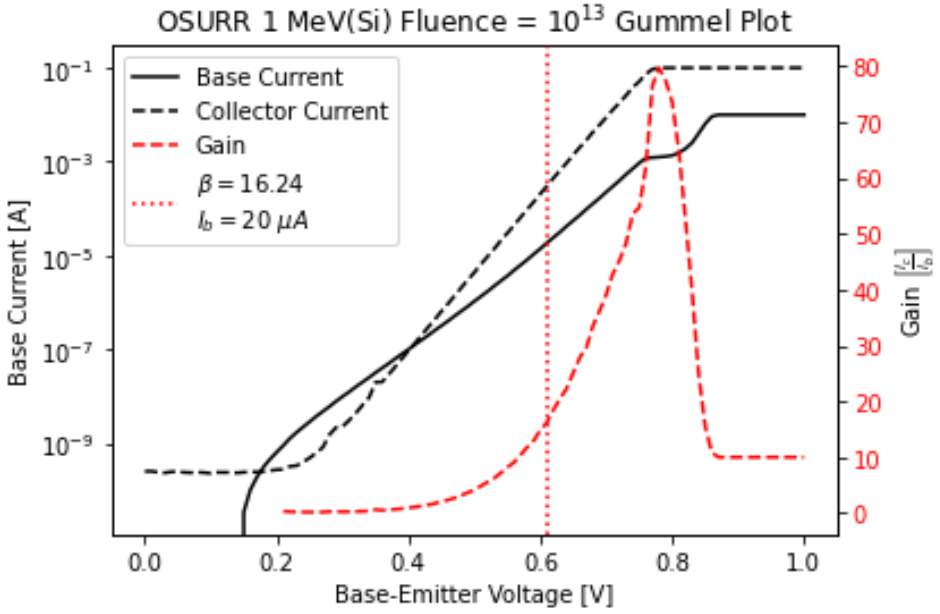

Figure 25: Gummel plot for the OSURR transistor irradiated at 10^{13} 1 MeV equivalent fluence.

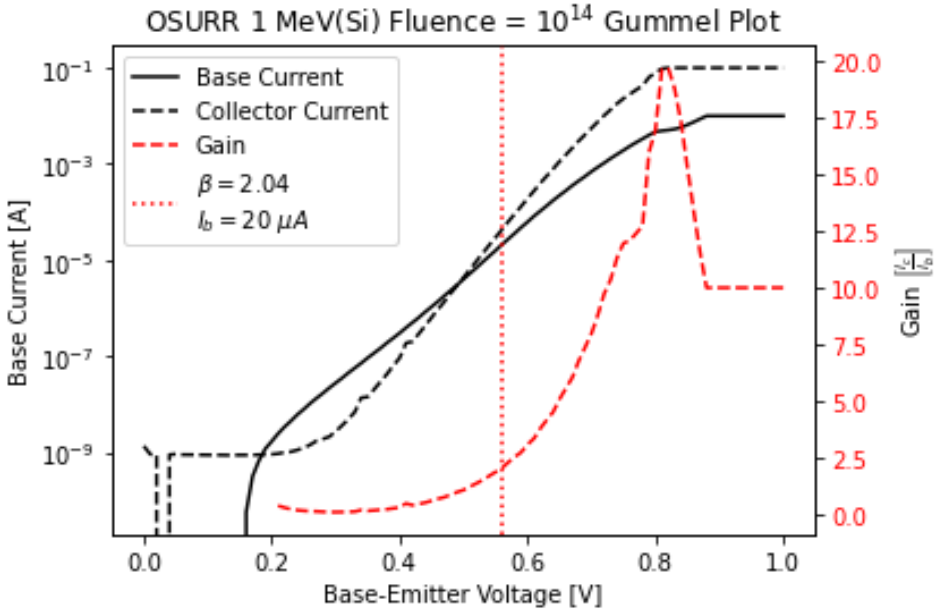

Figure 26: Gummel plot for the OSURR transistor irradiated at 10^{14} 1 MeV equivalent fluence.

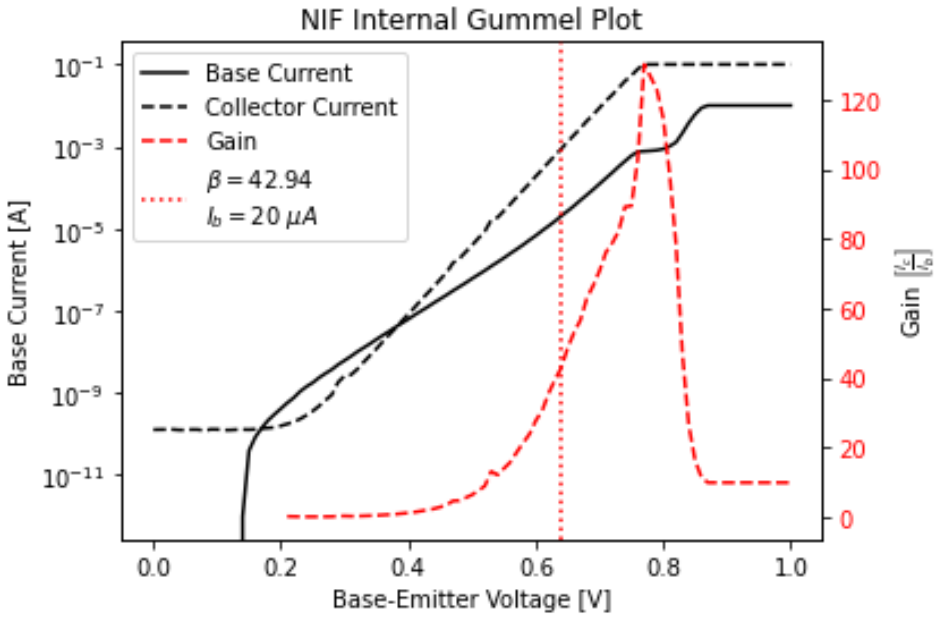

Figure 27: Gummel plot for the ATHENA internal irradiated device.

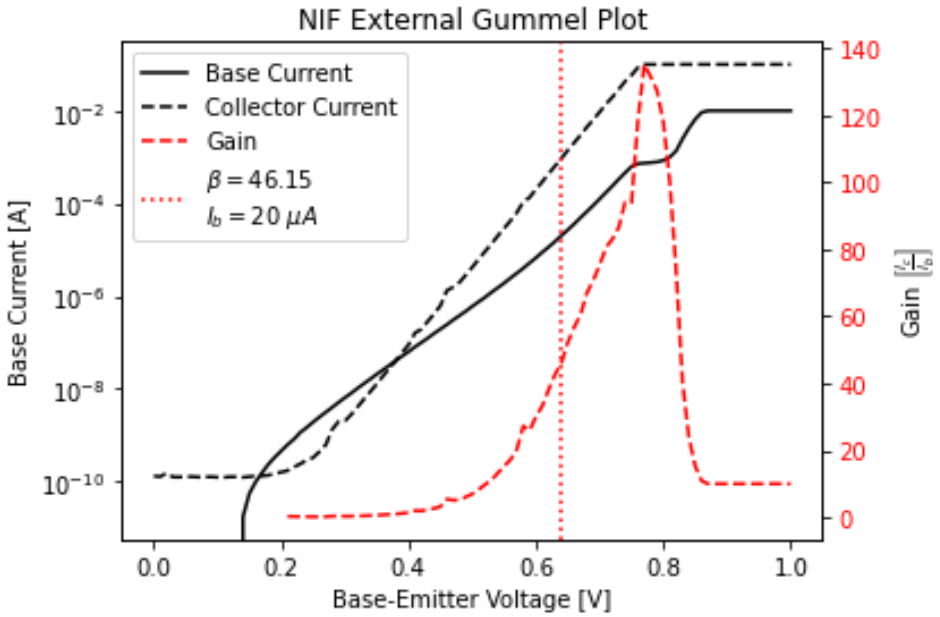

Figure 28: Gummel plot for the ATHENA external irradiated device.

Appendix B. Keithley 237 Operation Python Code

Code to operate the Keithley 237 SMU.

```
import os
import numpy as np
import matplotlib.pyplot as plt
import pandas as pd
import pyvisa
import time
import os, sys
fdir = os.path.dirname(__file__)

def connect():
    '''Connect to instruments'''

    rm = pyvisa.ResourceManager()
    print(rm.list_resources()) # LIST CONNECTED
       INSTRUMENTS
    my_instrument = input('Input␣instrument␣listing:␣') #
       INPUT INSTR ADDRESS
    my_instrument = rm.open_resource(my_instrument,
       open_timeout=1000)
    print(my_instrument.query("*IDN?")) # What are you?
    my_instrument.delay = 0.1

    return my_instrument
```

```
def settings(my_instrument):
    """
    Make settings for Keithley Source Measurement Unit and
        voltage sweep

    Inputs: my_instrument = instrument variable

    Outputs:
        VoltLow = Starting voltage for sweep
        VoltHigh = Final voltage for sweep
        step = step size
    """

    source = int(input(""" Input number of SOURCE
       selection below:
                        0) Voltage
                        1) Current

                           Input here: """))
    function = int(input(""" Input number of FUNCTION
       selection below:
                           0) DC
                           1) SWEEP

                              Input here: """))
    my_instrument.write('F%d,%dX'%(source, function))
```

```
    # DATA FORMAT
    my_instrument.write('G5,2,0X')

    # TRIGGER
    my_instrument.write('T1,7,0,0X')
    my_instrument.write('R1X')


    # Input voltages
    VoltLow = input("Input␣lowest␣boundary␣for␣voltage␣
       sweep:␣")
    VoltLow = float(VoltLow)

    VoltHigh = input("Input␣highest␣boundary␣for␣voltage␣
       sweep:␣")
    VoltHigh = float(VoltHigh)

    step = input("Input␣voltage␣step␣size:␣")
    step = float(step)

    return VoltLow,VoltHigh,step

''' Connect and set initial settings CV analyzer'''
keithley = connect()
keithley.clear()
```

```
VoltLow,VoltHigh,step = settings(keithley)

tests = [] # List to store lists of samples
current = [] # List for average value of capacitance for
   each samples
voltage = [] # List for average value of voltages for each
    sample
V = np.arange(VoltLow,VoltHigh,step) # Sweep between low
   and high voltages provided in settings

# Build up homemade sweep
tic = time.perf_counter()

for i in V:
    samples = []
    a = f'B{i:.3f},1,0X'
    keithley.write(a)
    time.sleep(0.1)

    # for j in range(7):
    #      # Take measurement at voltage i
    keithley.write('N1X')
    M = keithley.query('H0X')
    print(M)
    time.sleep(0.1)
    keithley.write('N0X')
```

```
    M.replace('\r\n','')
    M = M.split(',')
    for i in range(len(M)):
        M[i] = float(M[i])
    voltage.append(M[0])
    current.append(M[1])
    #     if VoltLow > M[2] or M[2]> VoltHigh: #
       Discarding overload data
    #         continue
    #     samples.append(M) # Store measurement in vector
    # if not samples: # Discarding overload data
    #     continue
    # tests.append(samples) # Store j vector in list
    if int(i) == int(V[(int(len(V)/2))]):
        print('You\'re half way there!')
    if round(i,3) == round(V[int((len(V)*0.9))],3):
        print('SOON!')
toc = time.perf_counter()
print('ALL DONE! Time for measurement to complete: ',toc-
   tic)


# Take average of j measurements
# AveCurrent= [np.mean([tests[j][i][0] for i in range(len(
   tests[j]))]) for j in range(len(tests))]
# AveVoltage = [np.mean([tests[j][i][2] for i in range(len
   (tests[j]))]) for j in range(len(tests))]
```

```
# plt.plot(AveVoltage,AveCurrent)



# Create and save dataframe as CSV
IVd = {'Voltage':voltage,'Current':current,'Samples':tests
   }
IVdata = pd.DataFrame(IVd)
IVdata.to_csv(fdir+r'\TESTTESTTEST.csv', index = False)
```

Appendix C. DEVSIM

3.1 Depletion width calculations

Constants:

$$k = 1.38 * 10^{-23} \frac{J}{K}$$

$$T = 300K$$

$$q = 1.6 * 10^{-19} C$$

$$K_s = 11.8$$

$$\epsilon_0 = 8.85 * 10^{-14} \frac{F}{cm}$$

Doping:

$$N_e = 10^{18} cm^{-3}$$

$$N_b = 10^{16} cm^{-3}$$

$$N_c = 10^{15} cm^{-3}$$

Built-in Voltage:

$$V_{bi} = \frac{kT}{q} ln\left(\frac{N_A N_D}{n_i^2}\right)$$

$$V_{biBC} = 0.656V$$

$$V_{biBE} = 0.835V$$

Depletion Width:

$$x_n = \sqrt{\frac{2K_s\epsilon_0}{q}\left(\frac{N_A}{N_D(N_A + N_D}\right)V_{bi}}$$

$$x_{nBC} = 8.82 * 10^{-5} cm$$

$$x_{nBE} = 3.28 * 10^{-7} cm$$

$$x_p = \frac{N_D x_n}{N_A}$$

$$x_{pBC} = 8.82 * 10^{-6} cm$$

$$x_{pBE} = 3.28 * 10^{-5} cm$$

$$W = x_n + x_p$$

$$W_{BC} = 9.71 * 10^{-5} cm$$

$$W_{BE} = 3.32 * 10{-}5 cm$$

3.2 Additional Figures

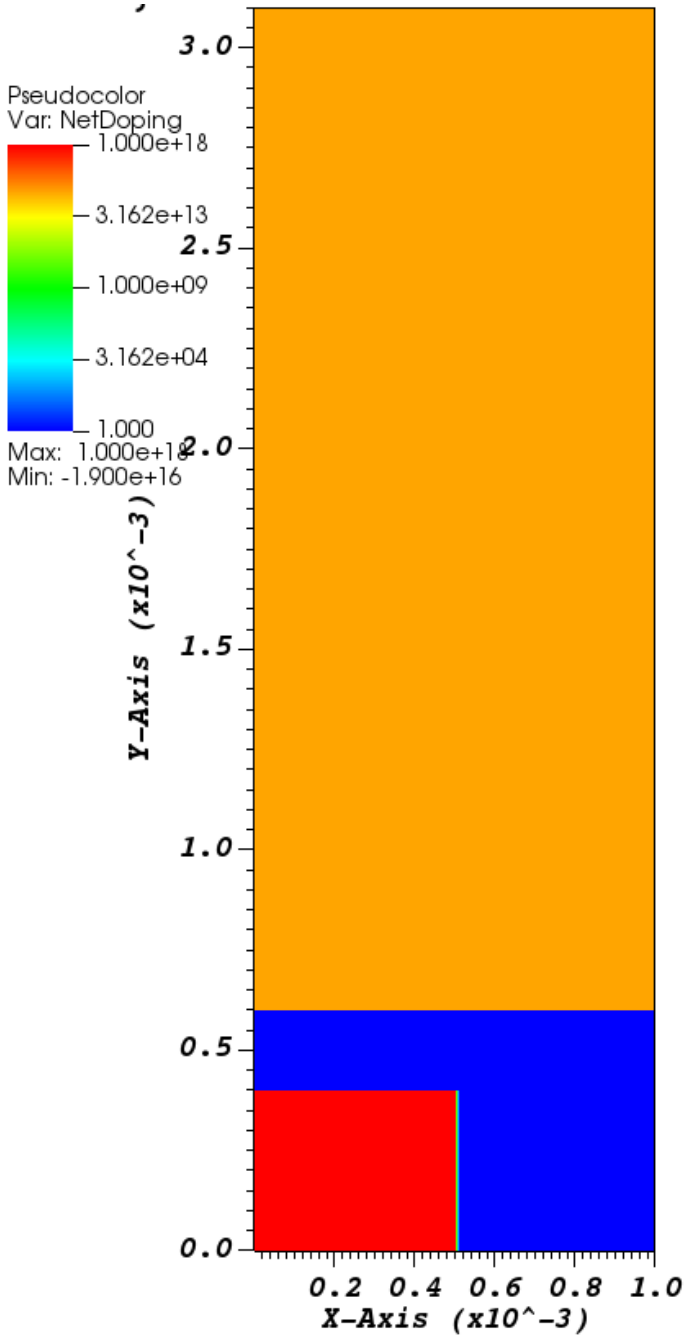

Figure 29: DEVSIM BJT net doping profile without the mesh in place. The simulation has a highly n doped emitter, p doped base, and low n doped collector.

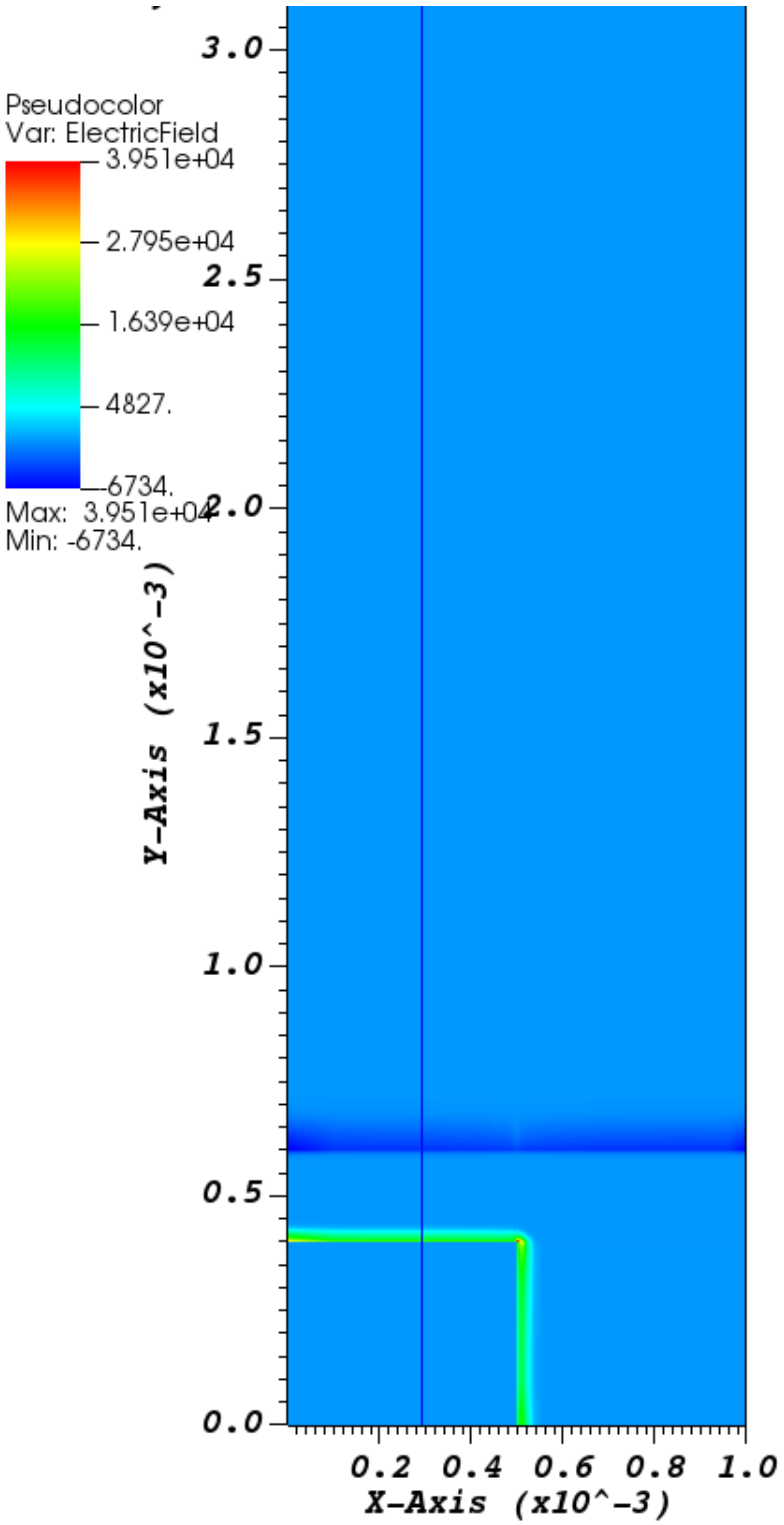

Figure 30: Electric field calculated in DEVSIM model. Edges of emitter, base, and collector regions can be clearly seen distinguished by the E-field between differently doped regions.The dark blue vertical line marks x=3 µm where the electric field is calculated for Figure 31.

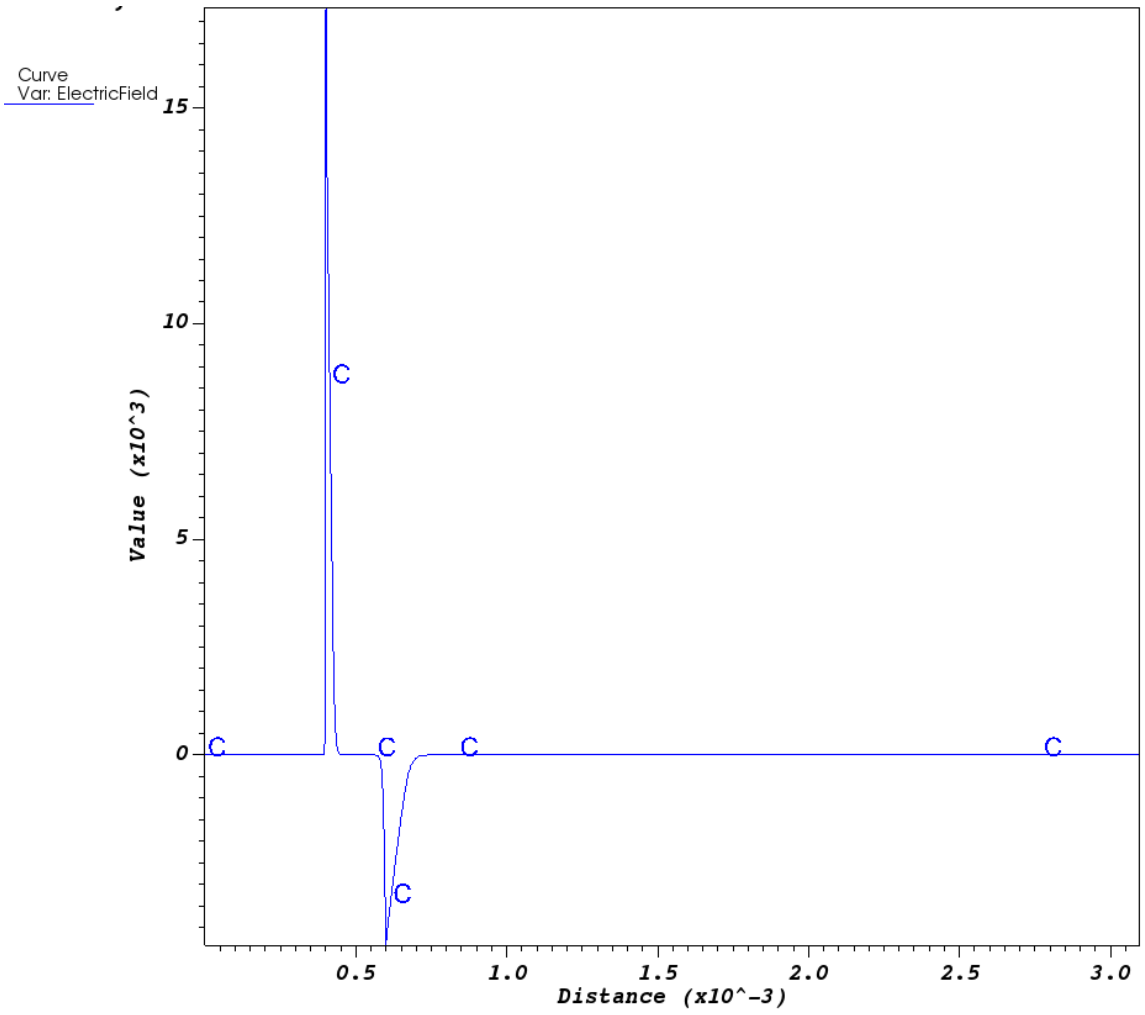

Figure 31: Electric field calculated in DEVSIM model in one dimension along the line x=3 µm. A positive electric field exists between the emitter and base and a negative field between the base and collector.

3.3 DEVSIM Simulation Python Code

Three Python scripts make up the DEVSIM simulation.

3.3.1 properties.py

properties.py sets the parameters for silicon using DEVSIM defaults and defines the doping profile and initial solutions for the device

```
'''
Defining properties for material and device
'''
from devsim import *
from devsim.python_packages.simple_physics import *

def SetParameters(device, region):
    '''
      Set parameters for 300 K
    '''
    SetSiliconParameters(device, region, 300)



def SetNetDoping(device, emitterdoping=1e18, basedoping=1
   e16, collectordoping=1e15):
    '''
      NetDoping
    '''

    # DOPING
```

```
    # # DISCRETE BJT
    CreateNodeModel(device, "bjt", "Acceptors", f"({
       basedoping}*step(y-4e-4)*step(6e-4-y) + {basedoping
       }*step(x-5e-4)*step(4e-4-y))")
    CreateNodeModel(device, "bjt", "Donors", f"({
       collectordoping}*step(y-6e-4) + {emitterdoping}*
       step(5e-4-x)*step(4e-4-y))")
    CreateNodeModel(device, "bjt", "NetDoping", "Donors-
       Acceptors")

    # # LINEAR BJT
    # CreateNodeModel(device, "bjt", "Acceptors", f"{
       basedoping}*step(y-5e-6)*step(50e-6-y)")
    # CreateNodeModel(device, "bjt", "Donors", f"{
       collectordoping}*step(y-50e-6) + {emitterdoping}*
       step(5e-6-y)")
    # CreateNodeModel(device, "bjt", "NetDoping", "Donors-
       Acceptors")



def InitialSolution(device, region, circuit_contacts=None)
   :
    # Create Potential, Potential@n0, Potential@n1
    CreateSolution(device, region, "Potential")
```

```
    # Create potential only physical models
    CreateSiliconPotentialOnly(device, region)


    # Set up the contacts applying a bias
    for i in get_contact_list(device=device):
        if circuit_contacts and i in circuit_contacts:
            CreateSiliconPotentialOnlyContact(device,
               region, i, True)
        else:
            ###print "FIX THIS"
            ### it is more correct for the bias to be 0,
               and it looks like there is side effects
            set_parameter(device=device, name=
               GetContactBiasName(i), value=0.0)
            CreateSiliconPotentialOnlyContact(device,
               region, i)

def DriftDiffusionInitialSolution(device, region,
   circuit_contacts=None):
    ####
    #### drift diffusion solution variables
    ####
    CreateSolution(device, region, "Electrons")
    CreateSolution(device, region, "Holes")
```

```
####
#### create initial guess from dc only solution
####
set_node_values(device=device, region=region, name="
   Electrons", init_from="IntrinsicElectrons")
set_node_values(device=device, region=region, name="
   Holes",     init_from="IntrinsicHoles")


###
### Set up equations
###
CreateSiliconDriftDiffusion(device, region)
for i in get_contact_list(device=device):
    if circuit_contacts and i in circuit_contacts:
        CreateSiliconDriftDiffusionAtContact(device,
           region, i, True)
    else:
        CreateSiliconDriftDiffusionAtContact(device,
           region, i)
```

3.3.2 mesh.py

mesh.py defines two types of mesh, a simple linear BJT and a discrete BJT. The discrete BJT was used for this thesis

```
'''
Defining properties of device mesh
```

```
'''

from devsim import *
from devsim.python_packages.simple_physics import *

def Create2DLinearMesh(device):
    ''' CREATES A SIMPLE LINEAR BJT '''
    create_2d_mesh(mesh=device)

    # DIMENSIONS
    emitterw = 5e-6
    basew = 45e-6
    collectorw = 100e-6
    thickness = 100e-6

    xmin = 0
    emitterxmax = thickness
    xmax = thickness
    ymin = 0
    emitterymax = emitterw
    baseymax = emitterw+basew
    ymax = emitterw+basew+collectorw

    # OUTLINE MESH
    add_2d_mesh_line(mesh=device, dir="x", pos=-1e-6, ps=1
       e-6)
```

```
add_2d_mesh_line(mesh=device, dir="x", pos=xmin, ps=5e
   -6)
# add_2d_mesh_line(mesh=device, dir="x", pos=
   emitterxmax, ps=1e-7)
add_2d_mesh_line(mesh=device, dir="x", pos=xmax, ps=5e
   -6)

add_2d_mesh_line(mesh=device, dir="y", pos=ymin, ps=1e
   -6)
add_2d_mesh_line(mesh=device, dir="y", pos=emitterymax
   , ps=1e-7)
add_2d_mesh_line(mesh=device, dir="y", pos=(baseymax-
   emitterymax)/2+emitterymax, ps=1e-6)
add_2d_mesh_line(mesh=device, dir="y", pos=baseymax,
   ps=1e-7)
add_2d_mesh_line(mesh=device, dir="y", pos=ymax, ps=5e
   -6)

add_2d_mesh_line(mesh=device, dir="y", pos=-1e-6, ps=1
   e-6)
add_2d_mesh_line(mesh=device, dir="y", pos=ymax+1e-6,
   ps=1e-6)

# add_2d_region(mesh=device, region="Emitter",
   material="Silicon", xl=xmin, xh=emitterxmax, yl=
   ymin, yh=emitterymax)
```

```
# add_2d_region(mesh=device, region="Base1", material
  ="Silicon", xl=emitterxmax, xh=xmax, yl=ymin, yh=
  emitterymax)
# add_2d_region(mesh=device, region="Base2", material
  ="Silicon", xl=xmin, xh=xmax, yl=emitterymax, yh=
  baseymax)
# add_2d_region(mesh=device, region="Collector",
  material="Silicon", xl=xmin, xh=xmax, yl=baseymax,
  yh=ymax)

# CREATE REGIONS
add_2d_region(mesh=device, region="bjt", material="
  Silicon", xl=xmin, xh=xmax, yl=ymin, yh=ymax)

# CONTACTS MUST HAVE A REGION ON ALL SIDES "AIR"
  SURROUNDS THE BJT
add_2d_region(mesh=device, region="air1", material="
  gas", yl=-1e-6, yh=0, xl=0, xh=xmax)
add_2d_region(mesh=device, region="air2", material="
  gas", yl=ymax, yh=ymax+1e-6, xl=0, xh=xmax)
add_2d_region(mesh=device, region="air3", material="
  gas", xl=-1e-6, xh=0)

# CREATE CONTACTS
add_2d_contact(mesh=device, name="Emitter", region="
  bjt", material="metal", yl=0, yh=0, xl=5e-6, xh=
```

```
        xmax-5e-6, bloat=1e-10)
    add_2d_contact(mesh=device, name="Collector", region="
        bjt", material="metal", yl=ymax, yh=ymax, xl=5e-6,
        xh=xmax-5e-6, bloat=1e-10)
    add_2d_contact(mesh=device, name="Base", region="bjt",
         material="metal", yl=(baseymax-emitterymax)/2+
        emitterymax-2e-6, yh=(baseymax-emitterymax)/2+
        emitterymax+2e-6, xl=0, xh=0, bloat=1e-10)

    # CREATE DEVICE
    finalize_mesh(mesh=device)
    create_device(mesh=device, device=device)

def Create2DDiscreteMesh(device):
    ''' CREATES A DISCRETE BJT '''
    create_2d_mesh(mesh=device)

    # DIMENSIONS

    emitterw = 4e-4
    basew = 2e-4
    collectorw = 25e-4
    thickness = 10e-4

    xmin = 0
    emitterxmax = thickness/2
```

```
xmax = thickness
ymin = 0
emitterymax = emitterw
baseymax = emitterw+basew
ymax = emitterw+basew+collectorw

# OUTLINE MESH
add_2d_mesh_line(mesh=device, dir="x", pos=xmin, ps=1e
   -4)
add_2d_mesh_line(mesh=device, dir="x", pos=emitterxmax
   , ps=1e-5)
add_2d_mesh_line(mesh=device, dir="x", pos=xmax, ps=1e
   -4)

add_2d_mesh_line(mesh=device, dir="y", pos=ymin, ps=1e
   -4)
add_2d_mesh_line(mesh=device, dir="y", pos=emitterymax
   , ps=1e-6)
add_2d_mesh_line(mesh=device, dir="y", pos=(baseymax-
   emitterymax)/2+emitterymax, ps=1e-5)
add_2d_mesh_line(mesh=device, dir="y", pos=baseymax,
   ps=1e-6)
add_2d_mesh_line(mesh=device, dir="y", pos=ymax, ps=2e
   -4)
```

```
add_2d_mesh_line(mesh=device, dir="y", pos=-1e-6, ps=1
   e-6)
add_2d_mesh_line(mesh=device, dir="y", pos=ymax+1e-6,
   ps=1e-6)

# CREATE REGIONS
add_2d_region(mesh=device, region="bjt", material="
   Silicon", xl=xmin, xh=xmax, yl=ymin, yh=ymax)

add_2d_region(mesh=device, region="air1", material="
   gas", yl=-1e-6, yh=0, xl=0, xh=xmax)
add_2d_region(mesh=device, region="air2", material="
   gas", yl=ymax, yh=ymax+1e-6, xl=0, xh=xmax)

# CREATE CONTACTS
add_2d_contact(mesh=device, name="Emitter", region="
   bjt", material="metal", yl=0, yh=0, xl=emitterxmax
   /2-1e-4, xh=emitterxmax/2+1e-4, bloat=1e-10)
add_2d_contact(mesh=device, name="Base", region="bjt",
    material="metal", yl=0, yh=0, xl=emitterxmax+(xmax
   -emitterxmax)/2-1e-4, xh=emitterxmax+(xmax-
   emitterxmax)/2+1e-6, bloat=1e-10)
add_2d_contact(mesh=device, name="Collector", region="
   bjt", material="metal", yl=ymax, yh=ymax, xl=xmax
   /2-1e-4, xh=xmax/2+1e-4, bloat=1e-10)
```

```
    # CREATE DEVICE
    finalize_mesh(mesh=device)
    create_device(mesh=device, device=device)
```

3.3.3 sweep.py

sweep.py uses the other two scripts, to build the mesh and solve for the current during the sweep.

```
from devsim import *
import devsim.python_packages.simple_physics as
   simple_physics
import devsim.python_packages.ramp as ramp
import properties
import mesh
import numpy as np
import pandas as pd
import matplotlib.pyplot as plt

# Create initial mesh

device="bjt2d"
r="bjt"

mesh.Create2DDiscreteMesh(device)
contacts = get_contact_list(device="bjt2d")
print("Contacts:␣",contacts)
if "Base" not in contacts:
```

```
    raise ValueError("Base not here!")
elif "Emitter" not in contacts:
    raise ValueError("Emitter not here!")
elif "Collector" not in contacts:
    raise ValueError("Collector not here!")


properties.SetParameters(device, r)
set_parameter(device=device, region=r, name="taun", value
   =1e-6)
set_parameter(device=device, region=r, name="taup", value
   =1e-7)

collectordoping = 1e15
basedoping = 1e16
emitterdoping = 1e18

properties.SetNetDoping(device,collectordoping=
   collectordoping, basedoping=basedoping, emitterdoping=
   emitterdoping)

# Initial DC solution

properties.InitialSolution(device, r)

properties.DriftDiffusionInitialSolution(device, r)
```

```
for c in get_contact_list(device="bjt2d"):
    set_parameter(device=device, name=simple_physics.
       GetContactBiasName(c), value=0)

solve(type="dc", absolute_error=4e3, relative_error=1e-5,
   maximum_iterations=100)

write_devices(file="bjt2d.dat", type="tecplot")

# RAMP COLLECTOR TO 3.5 VOLTS BY 0.5 V STEPS
Vc = np.linspace(0,3.4,7)
Ic = []
Ib = []
Ie = []
for v in Vc:
    set_parameter(device=device, name=simple_physics.
       GetContactBiasName("Collector"), value=float(v))
    try:
        solve(type="dc", absolute_error=4e3,
           relative_error=1e-7, maximum_iterations=50)
        Ic.append(get_contact_current(device="bjt2d",
           contact="Collector",equation="
           HoleContinuityEquation")+get_contact_current(
           device="bjt2d",contact="Collector",equation="
           ElectronContinuityEquation"))
```

```
        Ib.append(get_contact_current(device="bjt2d",
           contact="Base",equation="HoleContinuityEquation
           ")+get_contact_current(device="bjt2d",contact="
           Base",equation="ElectronContinuityEquation"))
        Ie.append(get_contact_current(device="bjt2d",
           contact="Emitter",equation="
           HoleContinuityEquation")+get_contact_current(
           device="bjt2d",contact="Emitter",equation="
           ElectronContinuityEquation"))
    except error:
        # save null values when solution does not converge
        Ic.append(np.nan)
        Ib.append(np.nan)
        Ie.append(np.nan)
# SAVE DEVICE IN THIS STATE FOR FUTURE RUNS
write_devices(file="bjt_collector34.dat", device="bjt2d",
   type="tecplot")
write_devices(file="bjt_collector34.msh", device="bjt2d",
   type="devsim")

def ramp(Vinit, Vfinal, steps, contact, savecurr):
    '''

    Parameters
    ----------
    Vinit : float
```

Starting Voltage.

Vfinal : float

Final Voltage.

steps : int

Number of steps.

contact : str

Contact to ramp.

savecurr : bool

Save currents to variable?.

Raises

Exception

DESCRIPTION.

Returns

Vr : Numpy array

Voltage ramped over

Ic : Numpy array

Current at collector.

Ib : Numpy array

Current at base.

Ie : Numpy array

Current at emitter.

df : Pandas DataFrame

```
    All of the above

'''
# RAMP BASE TO 1 V, RECORD CURRENT AT CONTACTS
Vr = np.linspace(Vinit, Vfinal, steps)
Ic = []
Ib = []
Ie = []
count = 0
for v in Vr:
    set_parameter(device=device, name=simple_physics.
       GetContactBiasName(contact), value=float(v))
    # try:
    solve(type="dc", absolute_error=1e10,
       relative_error=1e-7, maximum_iterations=50)
    print('\n SOLVED FOR V=%f \n'%v)
    simple_physics.PrintCurrents("bjt2d", "Base")
    Ic.append(get_contact_current(device="bjt2d",
       contact="Collector",equation="
       HoleContinuityEquation")+get_contact_current(
       device="bjt2d",contact="Collector",equation="
       ElectronContinuityEquation"))
    Ib.append(get_contact_current(device="bjt2d",
       contact="Base",equation="HoleContinuityEquation
       ")+get_contact_current(device="bjt2d",contact="
       Base",equation="ElectronContinuityEquation"))
```

```
    Ie.append(get_contact_current(device="bjt2d",
       contact="Emitter",equation="
       HoleContinuityEquation")+get_contact_current(
       device="bjt2d",contact="Emitter",equation="
       ElectronContinuityEquation"))
    count = 0

    # Raise error if more than 5 non-convergences in a
        row
    if count >= 5:
        raise Exception("Five non-converges in a row."
           )

# Convert current lists to Numpy arrays
Ic = np.asarray(Ic)
Ib = np.asarray(Ib)
Ie = np.asarray(Ie)

write_devices(file="bjt_base1.dat", device="bjt2d",
   type="tecplot")

# ACCOUNT FOR DEFAULT 5um THICKNESS OF DEVICE
Ic = Ic*5e-4 # cm
Ib = Ib*5e-4
Ie = Ie*5e-4
```

```
    data = {contact+"␣Voltage": Vr, "Collector␣Current":
       Ic, "Base␣Current": Ib, "Emitter␣Current": Ie}

    df = pd.DataFrame(data)

    if savecurr == True:
        return Vr, Ic, Ib, Ie

# BEGIN DATAFRAME FOR DATA
lifetime_n = [1e-6, 1e-7, 1e-8, 1e-9]
mobility_n = [1200, 800, 400, 100]
lifetime_p = [1e-6, 1e-7, 1e-8, 1e-9]
mobility_p = [400, 300, 200, 100]

collector = {}
base = {}
gain20um = {}
data = {"Lifetime": [], "Mobility": [], "Gain": []}

# Loop through lifetimes
for tau in lifetime_n:
    set_parameter(device=device, region=r, name="tau_n",
       value=tau)
    solve(type="dc", absolute_error=1e10, relative_error=1
       e-7, maximum_iterations=50)
    idx = []
```

```
    # Loop through mobilities
    for mu in mobility_n:
        set_parameter(device=device, region=r, name="mu_n"
            , value=mu)
        Vr, Ic, Ib, Ie = ramp(0, 1, 101, "Base", True)

        collector[mu] = Ic
        base[mu] = Ib
        ramp(1, 0, 5, "Base", False)

        idx.append(np.argmin(np.abs(collector[mu]-2e-5)))
        gain20um[mu] = np.abs(collector[mu]/base[mu])[idx
            [-1]]

        print(f"Gain␣where␣Ic␣=␣20␣um␣and␣mobility␣=␣{mu}:
            ␣", gain20um[mu])
        data["Lifetime"].append(tau)
        data["Mobility"].append(mu)
        data["Gain"].append(gain20um[mu])
display(data)
```

Bibliography

1. Nicholas J. Quartemont, George Peterson, Colton Moran, Adib Samin, Buguo Wang, Charles Yeamans, Brandon Woodworth, Darren Holland, James C. Petrosky, and James E. Bevins. *Nuclear Instruments and Methods in Physics Research Section A: Accelerators, Spectrometers, Detectors and Associated Equipment*, (September):165777.

2. Defense Threat Reduction Agency. *Handbook of Nuclear Weapon Effects*. Belvoir, VA, 1996.

3. American Society for Testing and Materials. Standard Practice for Characterizing Neutron Energy Fluence Spectra in Terms of an Equivalent Monoenergetic Neutron Fluence for Radiation-Hardness Testing of Electronics, 2002.

4. Richard C. Jaeger and Travis N. Blalock. *Microelectronic Circuit Design*. McGraw-Hill, New York, 4 edition, 2011.

5. James Bevins, James Petrosky, Charles Yeamans, George Peterson, Darren Holland, and Adib Samin. Validation of Microelectronic Device Response Using Threat-Representative Neutron Environments Validation of Microelectronic Device Response Using Threat-Representative Neutron Environments. 2020.

6. E. Bielejec, G. Vizkelethy, N. R. Kolb, D. B. King, and B. L. Doyle. Damage Equivalence of Heavy Ions in Silicon Bipolar Junction Transistors. *IEEE Transactions on Nuclear Science*, 53(6):3681–3686, 2006.

7. E. Bielejec, G. Vizkelethy, R. M. Fleming, and D. B. King. Metrics for Comparison Between Displacement Damage Due to Ion Beam and Neutron Irradiation in Silicon BJTs. *IEEE Transactions on Nuclear Science*, 54(6):2282–2287, 2007.

8. George C. Messenger. Current Gain Degradation Due to Displacement Damage for Graded Base Transistors. *Proceedings of the IEEE*, 55(3):413–414, 1967.

9. Myo Min Oo, N. K.A. Md Rashid, J. Abdul Karim, M. R.Mohamed Zin, and N. F. Hasbullah. Neutron Radiation Effect on 2N2222 and NTE 123 NPN Silicon Bipolar Junction Transistors. *IOP Conference Series: Materials Science and Engineering*, 53(1), 2013.

10. G. Vizkelethy, E. Bielejec, R.M. Fleming, D.B. King, and B.L. Doyle. Comparison of Displacement Damage Due to Ion and Neutron Beam Irradiations in Silicon Bipolar Junction Transistors. In *18th International Conference on Ion Beam Analysis*, Hyderabad, India, 2007.

11. G.P. Summers, E.A. Burke, C.J. Dale, E.A. Wolicki, P.W. Marshall, and M.A. Gehlhausen. Correlation of Particle-Induced Displacement Damage in Silicon. *IEEE Transactions on Nuclear Science*, 34(6):1133–1139, 1987.

12. Patrick J Griffin. Rigorous Uncertainty Propagation Using a Dosimetry Transfer Calibration. 2017.

13. G.C. Messenger and J.P. Spratt. The Effects of Neutron Irradiation on Germanium and Silicon. In *Proceedings of the IRE*, volume 46, pages 1038–1044, 1958.

14. The Ohio State University. Research Reactor, 2022.

15. Olivia M Borman. Neutron Versus Gamma Radiation Effects on Ytterbium-doped Optical Fibers. 2016.

16. Nickolas A Duncan. Changes to Electrical Conductivity in Irradiated Carbon Nanocomposites. *Master's Thesis*, 2011.

17. E. Burgett, N. Hertel, T. Blue, J. Chenkovich, and J. Talnagi. Neutron Spectral Measurement of the Ohio State Research Reactor Pneumatic Tube. *Journal of Radioanalytical and Nuclear Chemistry*, 282(1):187–191, 2009.

18. Ohio State University. OSURR Rabbit Neutron Spectrum (450 kW), 2020.

19. Edward E. Conrad. Considerations in Establishing a Standard for Neutron Displacement Energy Effects in Semiconductors. *IEEE Transactions on Nuclear Science*, 18(6):200–205, 1971.

20. John G. Williams, Patrick J. Griffin, Donald B. King, David W. Vehar, Tim Schnauber, S. Michael Luker, and K. Russell De Priest. Simultaneous Evaluation of Neutron Spectra and 1-MeV-Equivalent (Si) Fluences at SPR-III and ACRR. *IEEE Transactions on Nuclear Science*, 54(6):2296–2302, 2007.

21. J Morin, J C Amoud, J David, P Zyromski, and C E A Valduc. Measuring 1 MeV (Si) Equivalent Neutron Fluences with PIN Silicon Diodes. pages 20–26, 1993.

22. S.M. Sze, Yiming Li, and Kwok K. Ng. *Physics of Semiconductor Devices*. John Wiley & Sons, Hoboken, NJ, fourth edition, 2021.

23. Robert F. Pierret. *Semiconductor Device Fundamentals*. Addison-Wesley Publishing Company, Inc., Natick, MA, 1996.

24. Myles Hollander, Douglas A. Wolfe, and Eric Chicken. *Nonparametric Statistical Methods*. John Wiley & Sons Inc., Hoboken, NJ, 3rd edition, 2014.

25. Joseph M Lawson. *A Comparative Analysis of Transmission Control Protocol Improvement Techniques over Space-Based Transmission Media*. PhD thesis, Air Force Institute of Technology, 2006.

26. Charles B Yeamans and Brent E Blue. National Ignition Facility Neutron Sources. *Llnl-Conf-739397*, pages 1–4, 2018.

27. Ohio State University. Pneumatic Transport System (PTS) / Rabbit Facility, 2022.

28. Juan E. Sanchez. DEVSIM Manual. 2021.

29. James C. Petrosky and Charles B. Yeamans. Neutron Source Development for National Security Applications Experiments. 2022.

30. Charles B. Yeamans. High Fluence 14 MeV Neturon Exposure Capability at the NIF, 2020.

REPORT DOCUMENTATION PAGE

Form Approved
OMB No. 0704–0188

1. REPORT DATE *(DD–MM–YYYY)*	2. REPORT TYPE	3. DATES COVERED *(From — To)*
26–03–2022	Master's Thesis	Sept 2020 — Mar 2022

4. TITLE AND SUBTITLE

NEUTRON SPECTRAL EFFECT ON
MICROELECTRONIC PERFORMANCE RESPONSE

5a. CONTRACT NUMBER

5b. GRANT NUMBER

F2DANX1013J101

5c. PROGRAM ELEMENT NUMBER

6. AUTHOR(S)

Mr. Wade Kloppenburg

5d. PROJECT NUMBER

5e. TASK NUMBER

5f. WORK UNIT NUMBER

7. PERFORMING ORGANIZATION NAME(S) AND ADDRESS(ES)

Air Force Institute of Technology
Graduate School of Engineering and Management (AFIT/EN)
2950 Hobson Way
WPAFB OH 45433-7765

8. PERFORMING ORGANIZATION REPORT NUMBER

AFIT-ENP-MS-22-M-098

9. SPONSORING / MONITORING AGENCY NAME(S) AND ADDRESS(ES)

115 Wyoming Blvd. SEe
Albuquerque, NM 87116
Email: clark.allred@us.af.mil

10. SPONSOR/MONITOR'S ACRONYM(S)

AFNWC

11. SPONSOR/MONITOR'S REPORT NUMBER(S)

12. DISTRIBUTION / AVAILABILITY STATEMENT

DISTRIBUTION STATEMENT A:

13. SUPPLEMENTARY NOTES

14. ABSTRACT

Response of 2N2222 bipolar junction transistors to neutrons from a pulsed thermonuclear or pulsed fission source are researched. Measurements used for comparing performance included the base-collector junction current-voltage and capacitance-voltage characteristics and device gain degradation. Little change was detected in steady-state operation of the base-collector junction, but evidence in the dynamic and capacitance measurements establish effects based on environment. Experimental results are compared to literature results and parameters are explored using a device model simulation code.

15. SUBJECT TERMS

Neutron damage, radiation effects, radiation hardness, microelectronics, bipolar junction transistors

16. SECURITY CLASSIFICATION OF:			17. LIMITATION OF ABSTRACT	18. NUMBER OF PAGES	19a. NAME OF RESPONSIBLE PERSON
a. REPORT	b. ABSTRACT	c. THIS PAGE			James C. Petrosky
Unclass	Unclass	Unclass	N/A	94	19b. TELEPHONE NUMBER *(include area code)* (937) 255-3636